Geosci. Model Dev. Discuss., https://doi.org/10.5194/gmd-2017-155
Manuscript under review for journal Geosci. Model Dev.
Discussion started: 7 September 2017

Geoscientific Model Development Discussions

ORCHIDEE-PEAT (revision 4596), a model for northern peatland CO_2, water and energy fluxes on daily to annual scales

Chunjing Qiu[1], Dan Zhu[1], Philippe Ciais[1], Bertrand Guenet[1], Gerhard Krinner[2], Shushi Peng[3], Mika Aurela[4], Christian Bernhofer[5], Christian Brümmer[6], Syndonia Bret-Harte[7], Housen Chu[8], Jiquan Chen[9], Ankur R Desai[10], Jiří Dušek[11], Eugénie S. Euskirchen[7], Krzysztof Fortuniak[12], Lawrence B. Flanagan[13], Thomas Friborg[14], Mateusz Grygoruk[15], Sébastien Gogo[16,17,18], Thomas Grünwald[5], Birger U. Hansen[14], David Holl[19], Elyn Humphreys[20], Miriam Hurkuck[6], Gerard Kiely[21], Janina Klatt[22], Lars Kutzbach[19], Chloé Largeron[1,23], Fatima Laggoun-Défarge[16, 17, 18], Magnus Lund[24] , Peter M. Lafleur[25], Xuefei Li[26], Ivan Mammarella[26], Lutz Merbold[27], Mats B. Nilsson[28], Janusz Olejnik[29,30], Mikaell Ottosson-Löfvenius[28], Walter Oechel[31], Frans-Jan W. Parmentier[32,33], Matthias Peichl[28], Norbert Pirk[34], Olli Peltola[26], Włodzimierz Pawlak[12], Corinna Rebmann[35], Daniel Rasse[36], Janne Rinne[34], Gaius Shaver[37], Hans Peter Schmid[22], Matteo Sottocornola[38], Rainer Steinbrecher[22], Torsten Sachs[39], Marek Urbaniak[29], Donatella Zona[30,40], Klaudia Ziemblinska[29]

1. Laboratoire des Sciences du Climat et de l'Environnement, UMR8212, CEA-CNRS-UVSQ F-91191 Gif sur Yvette, France
2. CNRS, Université Grenoble Alpes, Institut de Géosciences de l'Environnement (IGE), F-38000 Grenoble, France
3. Department of Ecology, College of Urban and Environmental Sciences, Peking University, 100871 Beijing, China
4. Finnish Meteorological Institute, Climate Change Research, FI-00101 Helsinki, Finland
5. Technische Universität (TU) Dresden, Institute of Hydrology and Meteorology, Chair of Meteorology, D-01062 Dresden, Germany
6. Thünen Institute of Climate-Smart Agriculture, Bundesallee 50, 38116 Braunschweig, Germany
7. Institute of Arctic Biology, University of Alaska Fairbanks, AK 99775 Fairbanks, USA
8. Department of Environmental Science, Policy, and Management, University of California, Berkeley, 94720, CA, USA
9. Center for Global Change and Earth Observations, Michigan State University, East Lansing, MI 48823, USA
10. Department of Atmospheric and Oceanic Sciences, University of Wisconsin–Madison, WI 53706 Madison, USA
11. Department of Matters and Energy Fluxes, Global Change Research Institute, Czech Academy of Sciences, 603 00 Brno, Czech Republic
12. Department of Meteorology and Climatology, University of Łódź, Narutowicza 88, 90-139 Łódź, Poland
13. Department of Biological Sciences, University of Lethbridge, Lethbridge, T1K 3M4 Alberta, Canada
14. Department of Geosciences and Natural Resource Management, University of Copenhagen, Oester Voldgade 10, 1350 Copenhagen K, Denmark
15. Department of Hydraulic Engineering, Warsaw University of Life Sciences—SGGW, Nowoursynowska 159, 02-776 Warszawa, Poland

Geosci. Model Dev. Discuss., https://doi.org/10.5194/gmd-2017-155
Manuscript under review for journal Geosci. Model Dev.
Discussion started: 7 September 2017

Geoscientific Model Development Discussions

16. Université d'Orléans, ISTO, UMR 7327, 45071 Orléans, France
17. CNRS, ISTO, UMR 7327, 45071 Orléans, France
18. BRGM, ISTO, UMR 7327, BP 36009, 45060 Orléans, France
19. Institute of Soil Science, Center for Earth System Research and Sustainability (CEN), Universität Hamburg, Germany
20. Department of Geography and Environmental Studies, Carleton University, K1S5B6 Ottawa, Canada
21. Department of Civil and Environmental Engineering, University College Cork, Cork, Ireland
22. Karlsruhe Institute of Technology, Institute of Meteorology and Climate Research, Atmospheric Environmental Research (IMK–IFU), 82467 Garmisch-Partenkirchen, Germany
23. CNRS and Univ. Grenoble Alpes, Institut de Géosciences de l'Environnement (IGE), 38000 Grenoble, France
24. Department of Bioscience, Arctic Research Centre, Aarhus University, 4000 Roskilde, Denmark
25. School of the Environment - Geography, Trent University, Peterborough, Ontario, K9J 7B8, Canada
26. Department of Physics, University of Helsinki, 00014 Helsinki, Finland
27. Mazingira Centre, International Livestock Research Institute (ILRI), 00100 Nairobi, Kenya
28. Department of Forest Ecology and Management, Swedish University of Agricultural Sciences, S-90183 Umeå, Sweden
29. Department of Meteorology, Poznań University of Life Sciences, 60-649 Poznań, Poland
30. Department of Matter and Energy Fluxes, Global Change Research Center, AS CR, v.v.i. Belidla 986/4a, 603 00 Brno, Czech Republic
31. Department of Biology, San Diego State University, CA 92182 San Diego,USA
32. The Arctic University of Norway, Institute for Arctic and Marine Biology, Postboks 6050 Langnes, 9037 Tromsø, Norway
33. Department of Geosciences, University of Oslo, Postboks 1022 Blindern, 0315, Oslo, Norway
34. Department of Physical Geography and Ecosystem Science, Lund University, 22362 Lund, Sweden
35. UFZ-Helmholtz Centre for Environmental Research, 04318 Leipzig, Germany
36. Norwegian Institute of Bioeconomy Research, Oslo, Akershus, Norway
37. Marine Biological Laboratory, The Ecosystems Center, Woods Hole, 02543 Massachusetts, USA
38. Department of Science, Waterford Institute of Technology, Waterford, Ireland
39. Helmholtz Centre Potsdam, GFZ German Research Centre for Geosciences, 14473 Potsdam, Germany
40. Department of Animal and Plant Sciences, University of Sheffield, Western Bank, Sheffield S10 2TN, UK

Correspondence to: Chunjing Qiu (chunjing.qiu@lsce.ipsl.fr)

Geosci. Model Dev. Discuss., https://doi.org/10.5194/gmd-2017-155
Manuscript under review for journal Geosci. Model Dev.
Discussion started: 7 September 2017

Geoscientific Model Development Discussions

Abstract

Peatlands store substantial amount of carbon, are vulnerable to climate change. To predict the fate of carbon stored in peatlands, the complex interactions between water, peat and vegetations need more attention. This study describes a modified version of the ORCHIDEE land surface model for simulating the hydrology, surface energy and CO_2 fluxes of peatlands on daily to annual time scales. The model, referred to as ORCHIDEE-PEAT, includes a separate soil tile in each 0.5 ° grid-cell, defined from a global peatland map and identified with peat-specific soil hydraulic properties. Runoff from non-peat vegetation with a grid-cell containing a fraction of peat is routed to this peat soil tile, which maintains shallow water tables. The water table position separates oxic from anoxic decomposition. The model is evaluated against eddy-covariance (EC) observations from 30 northern peatland sites, with the maximum rate of carboxylation (V_{cmax}) being optimized at each site to match the peak of growing season gross primary productivity (GPP), derived from direct EC measurements. Regarding short-term variations from day to day, the model performance was good for the variations in GPP (r^2 = 0.76, Nash-Sutcliff modeling efficiency, MEF = 0.76), with lesser accuracy for latent heat fluxes (LE, r^2 = 0.42, MEF = 0.14) and Net ecosystem CO_2 exchange (NEE, r^2 = 0.38, MEF = 0.26). Seasonal variations in GPP, NEE and energy fluxes on monthly scales showed moderate to high r^2 values ranging from 0.57 to 0.86. For spatial across-sites gradients of annual mean GPP, NEE and LE, r^2 of 0.93, 0.27, and 0.71, respectively, were achieved. The water table variations are not well predicted (r^2 < 0.1), likely due to the uncertain water input to the peat from surrounding areas. However, when using the observed water table in the carbon module to define the fraction of oxic and anoxic decomposition instead of the modeled water table, ORCHIDEE-PEAT shows a small improvement in reproducing NEE. Moreover, we found a significant relationship between optimized V_{cmax} and the latitude (temperature), which can better reflect the spatial gradients of annual NEE than using an average V_{cmax} value. In a future version of ORCHIDEE-PEAT, the influences of water table on photosynthesis and depth-dependent influences of soil

113 temperature on respiration may be included.

114

115 **1. Introduction**

116 Peatlands cover only 3–5% of the Earth's land area, but store large amounts of soil
117 organic carbon. This carbon is primarily in the boreal and sub-arctic regions
118 (75–80%), while about 15% is in the tropical regions (Frolking et al., 2011; Page et al.,
119 2011). Current estimates of the northern peatland carbon stocks vary from 270 to 450
120 Pg C (Gorham, 1991; Turunen et al., 2002; Yu et al., 2010). Northern peat
121 accumulation occurred mainly during the Holocene, originating from plant litter
122 production exceeding decomposition in water-logged soil conditions, with low pH
123 and low temperatures (Parish et al., 2008). The future of the carbon stored in these
124 peatlands under the warmer environment and altered hydrological regimes is very
125 uncertain. Logically, higher CO_2 concentrations and elevated temperatures will
126 stimulate higher carbon uptake due to longer growing seasons and higher
127 photosynthetic rates (Aurela et al., 2004; Adkinson et al., 2011). However, the
128 accumulation is also coupled with a high evaporative demand that will lower the
129 ground water table, resulting in increased heterotrophic respiration rates (i.e., carbon
130 loss) (Mertens et al., 2001; Sulman et al., 2009; Adkinson et al., 2011). In addition to
131 the above potential climatic influences, other natural and anthropogenic disturbance
132 (permafrost melt, drainage, fires, etc.) can also play a role in determining the future
133 carbon balance of these vulnerable ecosystems (Turetsky et al., 2002; Parish et al.,
134 2008). Drainage and fires have particularly important impacts on the carbon balance
135 of the tropical peatlands (Page et al., 2002; Hooijer et al., 2010).

136 A number of peat carbon models have been reported in the literature. For example,
137 Frolking et al. (2010) created the Holocene Peat Model (HPM) which includes
138 feedbacks between plant communities, water table, peat properties, and peat
139 decomposition. This model was applied at Mer Bleue bog in southern Canada and
140 validated with data from peat-core observations. HPM is a long-term peat
141 accumulation model that works at an annual time step but cannot simulate seasonal

variations of key water processes in peatland. Wania et al. (2009a, 2009b) integrated peatlands and permafrost into the Lund-Potsdam-Jena model (LPJ-WHy), in their model, the upper 0.3 m of peatland soils (the acrotelm) experiences a fluctuating water table and the underlying layer (the catotelm) is inundated permanently. A constant soil moisture modifier (0.35) was used to reduce acrotelm decomposition. Spahni et al. (2013) adopted and improved LPJ-Why to take into account the effects of varying water table depth on acrotelm decomposition rates using a weighted average of the aerobic and anaerobic respiration modifier, and implemented a dynamic nitrogen cycle. In the dynamic global vegetation model (DGVM) CLIMBER2-LPJ, Kleinen et al. (2012) determined the fraction of oxic decomposition in the acrotelm by comparing the water table position and the acrotelm height. Chaudhary et al. (2016, 2017) included a dynamic multi-layer peat accumulation functionality in a customized Arctic version of the Lund-Potsdam-Jena General Ecosystem Simulator (LPJ-GUESS). In their approach, new layers of litter were added at the top of the soil every year, and the remaining litter mass after decomposition was treated as a new individual peat layer from the first day of the following year. The decomposition rate of peat, modulated by temperature and moisture, declined over time. In these four peatland models, the water table depth is calculated from a bucket model. In the context of Earth System Modeling, the land surface is tend to be represented by several multi-layer schemes, such as multi-layer plant canopy and root, multi-layer snow, multi-level soil carbon and energy budgets (Best et al., 2011; Mcgrath et al., 2016; Zhu et al., 2016). To model peatlands consistently in land surface models, a multi-layer soil hydrology scheme is needed. Meanwhile, a more physics-based multi-layer scheme can provide more prognostic power in predicting peatland water table dynamics.

In this study, we presented the results of the development of a peat hydrology and carbon model in the ORCHIDEE land surface scheme, focusing on the water table dynamics and its effects on the energy budgets, and on carbon decomposition occurring within the oxic and the water-saturated part of the peat profile. CH_4 fluxes

Geosci. Model Dev. Discuss., https://doi.org/10.5194/gmd-2017-155
Manuscript under review for journal Geosci. Model Dev.
Discussion started: 7 September 2017

and DOC loss through runoff are important components of the carbon balance of a peatland (Chu et al., 2014; Olefeldt et al., 2012), but are not included in this study. The originality of this new peat model is that it is incorporated consistently into the land surface scheme in order to conserve water, carbon and energy at scales going from local sites to grid-based large-scale applications in an Earth System Modeling context. The model structure and equations are described in Sect. 2, and its evaluation against water table depth, energy and CO_2 fluxes measured in 30 northern peat sites is presented in Sect. 3.

2. Model description

2.1 General structure of the model

The ORCHIDEE land surface model simulates biophysical processes of rainfall interception, soil water transport, latent (LE) and sensible (H) heat fluxes, heat diffusion in the soil, and photosynthesis on a 30-min time step (Ducoudré et al., 1993). Carbon cycle processes such as carbon allocation, respiration, mortality, litter and soil carbon dynamics, are simulated on a daily time step (Krinner et al., 2005).

ORCHIDEE discretizes the vegetation into plant functional types (PFT): eight for trees, two for natural C3 and C4 grasses, two for C3 and C4 crops, and one as bare-soil type. Across the PFTs, plants are described with the same equations but different parameter values, except for leaf onset and senescence that follow PFT-specific equations (Botta et al., 2000). In grid-based simulations, PFTs are grouped into three soil tiles: one with bare soil, one with all tree PFTs, and one with all short vegetation. The water budget of each soil tile is calculated independently. The version of ORCHIDEE implemented in this study uses the same (dominant) soil texture for all the soil tiles of a grid cell to define the reference saturated hydraulic conductivity ($K_{s\text{-}ref}$), and the saturated and residual volumetric water contents (θ_s, θ_r). Dominant soil textural classes are taken from the Zobler's soil texture map (Zobler, 1986) at 1° resolution. The original five soil textures (fine, medium-fine, medium, medium-coarse, coarse) in Zobler's map are reduced to three (fine, medium, coarse),

Geosci. Model Dev. Discuss., https://doi.org/10.5194/gmd-2017-155
Manuscript under review for journal Geosci. Model Dev.
Discussion started: 7 September 2017

by grouping the medium-fine, medium, and medium-coarse into one class. Hydrological parameters of the three dominant soil textures are taken from Carsel and Parrish (1988) (Table 1).

Each soil tile in ORCHIDEE has eleven vertical layers (with a total depth of 2.0 m) with exponentially coarser vertical resolution (Fig. 1). The Fokker-Planck equation is used to describe the vertical diffusion of water in the soil. The Mualem (1976) - Van Genuchten (1980) model (Eq. 1 and 2) is used to define the hydraulic conductivity (K, m s^{-1}) and diffusivity (D, m^2 s^{-1}) as a function of volumetric water content (θ, m^3m^{-3}):

$$K(\theta) = K_s\sqrt{\theta_f}(1-(1-\theta_f^{1/m})^m)^2 \quad (1)$$

$$D(\theta) = \frac{(1-m)K(\theta)}{\alpha m}\frac{1}{\theta-\theta_r}\theta_f^{\frac{-1}{m}}(\theta_f^{\frac{-1}{m}}-1)^{-m} \quad (2)$$

where θ is the volumetric water content (m^3 m^{-3}), θ_s is the saturated water content (m^3 m^{-3}), θ_r is the residual water content (m^3 m^{-3}), θ_f is the relative water content and is calculated as $\theta_f = \frac{\theta-\theta_r}{\theta_s-\theta_r}$, K_s is the saturated hydraulic conductivity (m s^{-1}), α is the inverse of the air entry suction (m^{-1}), and *m* is a dimensionless parameter.

Following Orgeval (2006) and Orgeval et al. (2008), K_s exponentially decreases with soil depth (z) below z_{lim} = 30 cm ($F_d(z)$), while a root-fracturing factor increases K_s where roots are denser ($F_{root}(z)$):

$$K_s(z) = K_{s-ref} \times F_d(z) \times F_{root}(z) \quad (3)$$

with $F_d(z) = \min(\max(\exp(-f(z-z_{lim})),0.1),1)$, $F_{root}(z) = \prod_{j\epsilon c}\max\left(1,\left(\frac{K_s^{max}}{K_{s-ref}}\right)^{\frac{1-\alpha_j z}{2}}\right)^{f_j}$,

where $K_{s\text{-}ref}$ is the reference top-soil saturated hydraulic conductivity determined by soil texture (m s^{-1}), K_s^{max} is the value of the coarser (sandy) texture and equals 8.25 × 10^{-5} m s^{-1}, α_j is a root profile decay factor for PFT *j* with a coverage fraction f_j, and *c* is the soil tile to which PFT *j* was assigned to.

2.2 Modifications in ORCHIDEE-PEAT

To simulate peat, we: 1) modified the parameters of plants growing on peat, 2) added a new peat soil tile with specific peat soil hydraulic properties, and 3) changed the

decomposition of peat carbon as being controlled by saturated conditions, through the modeled water table (WT).

Modified peat plant parameters. As a response to the unique stress conditions in peatlands (i.e., oxygen deficit, nutrient limitation), peatland vegetation has shallow and extensive root systems (Boutin and Keddy, 1993; Iversen et al., 2015). In this study, a C3 grass peatland PFT with a rooting depth of 30 cm implemented by Largeron et al. (2017) was used. The maximum rate of carboxylation (V_{cmax}) typically varies across peat sites (Rennermalm et al., 2005; Bubier et al., 2011), and further varies with leaf nitrogen, phosphorus content, and specific leaf area (Wright et al., 2004; Walker et al., 2014). For instance, V_{cmax} value for *Sphagnum* at the Old Black Spruce site (53.985 °N, 105.12 °W) in Canada were 5, 14 and 6 μmol m^{-2} s^{-1} during spring, summer and autumn respectively, while that for *Pleurozium* were 7, 5, and 7 μmol m^{-2} s^{-1} (Williams and Flanagan, 1998). Bui (2013) conducted a fertilization experiment at the Mer Bleue Bog (Canada, 45.41 °N, 75.52 °W) on the dominant ericaceous shrub and reported that V_{cmax} values ranged between 6 and 179 μmol m^{-2} s^{-1}, with significantly higher V_{cmax} values after addition of nitrogen (6.4 g N m^{-2} $year^{-1}$) at 20 times the growing season ambient wet N deposition rate with or without phosphorus (P) and potassium (K). In this study, we used a default V_{cmax} value of 16 μmol m^{-2} s^{-1} for peat PFT, following a literature survey by Largeron et al. (2017). Later (Sect. 4.1), we calibrated V_{cmax} at each site so that modeled peak gross primary production (GPP) matched peak values derived from direct EC measurements, and then regressed this adjusted V_{cmax} value with environmental and climate variables. We note that this adjustment of V_{cmax} may over- or under-compensate for biases in other model parameters that impact maximum GPP, such as leaf area index (LAI), specific leaf area (SLA), canopy light absorption parameters, water and temperature stresses.

Peat-specific soils hydraulics. Peatlands generally occur in flat areas that are poorly drained and/or receive runoff and sub-surface water from the surrounding landscape (Graniero and Price, 1999). The low permeability catotelm peat layer is permanently saturated. In ORCHIDEE-PEAT, the new soil tile added in a grid cell to represent

Geosci. Model Dev. Discuss., https://doi.org/10.5194/gmd-2017-155
Manuscript under review for journal Geosci. Model Dev.
Discussion started: 7 September 2017

peatland as a landscape element was assumed to receive surface runoff from the other three soil tiles (bare soil, trees, grasses) and has a drainage flux reduced to zero (Largeron et al., 2017). Further, considering that the water table of a peatland can rise above the ground surface, an above surface water reservoir with a maximum height of 10 cm was added (Fig. 1b). This reservoir loses water to rivers when filled, and re-infiltrates into the peat soil on the next time step (Largeron et al., 2017). We verified that the measured standing water remained below 10 cm above the soil surface at 16 out of 20 northern peat sites where water table depth was recorded in this study (Table S1). The four exceptions were Winous Point North Marsh (US-WPT), Himmelmoor (DE-Hmm), an Alaska fen (US-Fen) and an Alaska bog (US-Bog), where observed water tables reached up to 77 cm, 39 cm, 46 cm and 34 cm above the soil surface, respectively.

Peat soils cannot be described with any of the mineral soil textures used for other tiles (Table 1) because the low bulk density and high porosity increase the downward water percolation (Rezanezhad et al., 2016). There is a large variability of observed peat saturated hydraulic conductivity (K) and diffusivity (D) in space, depth and time. This is partly related to the degree of decomposition and compression of organic matter (Gnatowski et al.,2010). Morris et al. (2015) reported near-surface saturated hydraulic conductivities (K) of 2.69×10^{-2} m s^{-1} to 7.16×10^{-6} m s^{-1} in bogs. Gnatowski et al. (2010) measured values of 5×10^{-6} m s^{-1} in a moss-covered peat, which is two orders of magnitude larger than in a woody peat (5.56×10^{-8} m s^{-1}). Peat hydraulic parameters values used in this study were applied after (Largeron et al., 2017), based on Letts et al. (2000) and Dawson (2006) (Table 1). The peat saturated hydraulic conductivity value of 2.45×10^{-5} m s^{-1} is comparable to the harmonic mean value (6×10^{-5} m s^{-1}) of Morris et al. (2015). The values of the other Van Genuchten parameters for peat (Table 1) are similar to those employed in other peatland models (Wania et al., 2009a; Wu et al., 2016).

Geosci. Model Dev. Discuss., https://doi.org/10.5194/gmd-2017-155
Manuscript under review for journal Geosci. Model Dev.
Discussion started: 7 September 2017

The peatland water table depth (WT, cm) is diagnosed by summing water heights in the eleven soil layers, calculated from the relative water content (Largeron et al., 2017):

$$WT = H_{tot} - \sum_{i=1}^{11}(\theta_{fi} * dz_i) - H_{ab}; \text{ with } \theta_{fi} = \frac{\theta_i - \theta_r}{\theta_s - \theta_r} , \quad (4)$$

where θ_{fi} is the relative volumetric water content of the i^{th} soil layer, θ_s is the saturated water content (m^3 m^{-3}), θ_r is the residual water content (m^3 m^{-3}), dz_i is the distance between node *i-1* and node *i* (Fig. 1, m), H_{tot} is the total soil column height being fixed to 2.0 m, and H_{ab} is the height of the water reservoir above soil surface (m). Thus, when the water table is above the surface, the modeled WT takes negative values.

Decomposition of peat carbon controlled by water saturation. In the standard version of ORCHIDEE, plant litter carbon is added to two litter pools: the metabolic and the structural pool. Decomposed litter carbon from these two pools is then distributed into three soil carbon pools: the active, slow and passive pool (Fig. S1), similar to the CENTURY model (Parton et al., 1988). Both temperature and moisture functions are used to control soil carbon decomposition rates (Text S1).

The original decomposition equations are combined with a new module to account for peat decomposition being controlled by water saturation, after Kleinen et al. (2012) (Fig. S1). Specifically, carbon from decomposed litter pools is added to the acrotelm carbon pool where it is then decomposed aerobically above the simulated water table, and anaerobically below it. The permanently saturated deep catotelm carbon pool receives a prescribed fraction (1.91% per year, Kleinen et al., 2012) of the acrotelm carbon, and is decomposed anaerobically at a very slow rate (3.35×10^{-5} yr^{-1}, Kleinen et al., 2012). Whereas acrotelm depth was fixed to 30 cm in some two-layer peat decomposition models (Yurova et al., 2007; Wania et al., 2009a; Spahni et al., 2013), we used the average of minimum summer water table position (WT_{min}) over the observational period to demarcate the boundary between the acrotelm and the catotelm at each site to take into account local site conditions. WT_{min} values were

Geosci. Model Dev. Discuss., https://doi.org/10.5194/gmd-2017-155
Manuscript under review for journal Geosci. Model Dev.
Discussion started: 7 September 2017

estimated based on current climate due to the lack of knowledge of initiation histories of these sites. For the long-term carbon accumulation estimations, the Holocene climate may be a better proxy since northern peatlands show peak initiation in the early Holocene (Yu et al., 2010). By comparing the height of the acrotelm (Fig. S1) with the WT depth, we derived the fraction of the acrotelm where carbon decomposes under oxic (β) vs. anoxic conditions (1-β). Acrotelm height was calculated from acrotelm carbon stock (C_A in Eq. 5-7), acrotelm carbon fraction ($C_{f,A}$) and acrotelm bulk density (ρ_A). Decomposition of peat carbon is then controlled by temperature and parameterized as an exponential function $Q_{10}\exp((T-T_{ref})/10\,℃)$ with $Q_{10} = 2.0$ and $T_{ref} = 30$ ℃ (Text S1). Soil carbon fluxes are given by:

$$F_{AC} = k_p C_A , \quad (5)$$

$$R_{A,o} = \beta k_A C_A , \quad (6)$$

$$R_{A,a} = (1-\beta)\mu k_A C_A , \quad (7)$$

$$R_C = k_C C_C , \quad (8)$$

where F_{AC} is the carbon flux from acrotelm to catotelm; $R_{A,o}$ is aerobically decomposed acrotelm carbon; $R_{A,a}$ is anaerobically decomposed acrotelm carbon; R_C is decomposed carbon in catotelm; C_A is carbon stored in the acrotelm; C_C is carbon stored in the catotelm; and β is the fraction of acrotelm under oxic conditions. A 10,100 years' spin-up was conducted to initialize peat depth at each site (Sect. 3.3). Following the study of Kleinen et al. (2012), the catotelm formation rate $k_p = 1.91 \times 10^{-2}\,yr^{-1}$, the acrotelm decomposition rate $k_A = 0.067\,yr^{-1}$, the catotelm decomposition rate $k_C = 3.35 \times 10^{-5}\,yr^{-1}$, the ratio of anaerobic to aerobic CO_2 production $\mu = 0.35$, carbon fraction in the acrotelm peat $C_{f,A} = 0.50$, the acrotelm density $\rho_A = 3.5 \times 10^4\,g\,m^{-3}$, carbon fraction in the catotelm peat $C_{f,C} = 0.52$, the catotelm density $\rho_C = 9.1 \times 10^4\,g\,m^{-3}$.

In the following analysis, carbon fluxes are defined positive if upwards. Thus,

Geosci. Model Dev. Discuss., https://doi.org/10.5194/gmd-2017-155
Manuscript under review for journal Geosci. Model Dev.
Discussion started: 7 September 2017

ecosystem respiration is positive, GPP is negative, and a negative NEE signifies the uptake of CO_2 by the ecosystem.

3. Validation of ORCHIDEE-PEAT at northern hemisphere peatland eddy-covariance sites

3.1 Sites description

To evaluate the performance of ORCHIDEE-PEAT in simulating CO_2, water and energy fluxes on daily to annual time scales among the peatlands, we compiled data from 30 northern peatland sites where eddy-covariance data and physical variables (water table, snow depth, soil temperature) were collected (Fig. 2, Table 2). These sites are spread between the temperate to the arctic climate zones, and include nine bogs and 18 fens. A marsh and two wet tundra sites (these two wet tundra sites are neither a fen nor a bog, hereafter they are referred to as 'tundra') with a ~30–50 cm thick organic layer are also included in this study. Among them, six sites are underlain by permafrost and one site is in a thermokarst area. The peatland fractional cover in the 0.5 °grid cell containing each site is from the Yu et al. (2010) map (Fig. 2, Table 2). A short description of all sites can be found in Supplementary Materials.

3.2 Meteorological forcing data

We ran the model for 29 different 0.5 ° grid cells corresponding to each peatland site (US-Fen and US-Bog are in the same grid cell, but their local meteorological data was different). Peatland fraction in each grid cell was prescribed from Yu et al. (2010), adapted by Largeron et al. (2017) to be matched with a high-resolution land cover map. For cells (15 out of 29) without peatland (Fig. 2, Table 2) in the large-scale map from Yu et al. (2010), a mean peatland fraction of 22% was assigned.

Time series of half-hourly air temperature, wind speed, wind direction, long-wave incoming radiation, short-wave incoming radiation, specific humidity, atmospheric pressure, and precipitation were used to drive ORCHIDEE-PEAT. All mentioned variables were from measurements made at each flux tower where CO_2 and energy

Geosci. Model Dev. Discuss., https://doi.org/10.5194/gmd-2017-155
Manuscript under review for journal Geosci. Model Dev.
Discussion started: 7 September 2017

(latent heat (LE) and sensible heat (H)) fluxes, water table position, soil temperature, and snow depth were recorded on a half-hourly time step. The linearly interpolated 6-hourly CRU-NCEP 0.5 ° global climate forcing dataset was used to fill the gaps. A linear correction was applied to meteorological forcing variables (except precipitation) in the CRU-NCEP dataset to match observations before gap-filling. For precipitation, no correction was applied. At CA-Wp2 and CA-Wp3, meteorological forcing data were measured only during the growing season, so CRU-NCEP data were linearly corrected using relationships derived from the available data. For some sites, several meteorological data were not measured, such as long-wave incoming radiation at NO-And, atmospheric pressure, short-wave incoming radiation, and long-wave incoming radiation at CZ-Wet. In these cases, CRU-NCEP data were used to fill the gaps without correction.

3.3 Model setup

ORCHIDEE-PEAT was first spun-up for 10,100 years, forced by the preindustrial atmospheric CO_2 concentration of 285 ppm, with repeated site-specific observational meteorological fields, and present-day vegetation fractions for each site. In reality, the climate changed through the Holocene, but since the initiation and climate history of each site are unknown, we assumed a constant present-day climate condition and peatland area. Thus this model is only suitable for simulating water, energy and CO_2 fluxes from peat on time scales ranging from days to decades. To accelerate the spin-up, ORCHIDEE-PEAT was first run for 100 years to reach the equilibrium for hydrology and soil thermal conditions, fast carbon pools and soil carbon input from dead plants. Then, a sub-model simulating only soil carbon dynamics (with fixed daily litter input from the previous simulation) was run for 10,000 years to accumulate soil carbon. Peatlands can reach equilibrium only when the addition of carbon equals carbon lost, which is attained on time scales of 10^4 years (Clymo, 1984; Wania et al., 2009b). The catotelm carbon pool in this study was still not fully equilibrated even after 10,100 years due to the low carbon decomposition rate in this reservoir (3.35 ×

395 10^{-5} yr^{-1}, Kleinen et al., 2012). The modeled peat carbon pool thus depends on the
396 time length of spin-up, which was fixed at 10,100 years. While in the real world, peat
397 age at some sites can be younger. For example, the sample from the second last 10 cm
398 peat segment at CA-Wp1 has an un-calibrated radiocarbon date of ~2200 years
399 (Flanagan and Syed, 2011). Since we focus on carbon and water fluxes on daily to
400 annual scales in this study, rather than on the simulation of peat carbon stocks, we
401 conducted a sensitivity analysis of modeled heterotrophic respiration to the length of
402 the spin-up, which shows only a slight increase of catotelm respiration with increasing
403 simulation time (Fig. S2). After the spin-up, transient simulations were conducted for
404 each site, forced by repeated site-specific climates and rising atmospheric CO_2
405 concentration during the period 1901-2015. Finally, the model outputs corresponding
406 to the respective measurement periods (all during 1999-2015) were compared to
407 observed time series for each site.

408 Two sets of simulations were conducted. In the first one (S1), soil water content
409 and water table position (WT) were modeled by ORCHIDEE-PEAT, and the WT was
410 used in the carbon module to define the fraction of oxic and anoxic decomposition in
411 the acrotelm. S1 was performed for all the 30 sites. In the second set (S2) of
412 simulations, we prescribed water table in the model to equal to observed values
413 (WT_{obs}). That is, soil moisture at layers below the measured water table was
414 prescribed as saturated ($\theta(z > WT_{obs}) = \theta_s$), while soil moisture above WT_{obs} was
415 simulated. WT_{obs} was further used in the carbon module in S2. S2 was performed only
416 for a subset of eight sites where at least two years of water table measurements were
417 available and where there were sufficient observations to gap-fill the WT_{obs} time
418 series (Table 2). For these sites, the gaps of WT_{obs} were filled with the mean value of
419 the same period from other years of measurement (Table S2). The simulation S2 was
420 designed to check if the model performance will improve (or deteriorate) when
421 prescribing WT exactly to its observed value, since WT is known to be a critical
422 variable impacting peat water and CO_2 exchange, and CH_4 emissions (Dušek et al.,
423 2009; Parmentier et al., 2011; Strack et al., 2006). Fixing the simulated water table to

Geosci. Model Dev. Discuss., https://doi.org/10.5194/gmd-2017-155
Manuscript under review for journal Geosci. Model Dev.
Discussion started: 7 September 2017

424 WT_{obs} in S2 violated the water mass conservation of the model but allowed us to
425 evaluate the carbon module independently from the hydrological module biases.
426
427 **3.4 Measures for evaluating model performance**
428 Following Jung et al. (2011) and Tramontana et al. (2016), we used site-specific daily
429 means, annual means, seasonal variations and daily anomalies to evaluate the model
430 performance. For each site, seasonal variations are calculated by removing the annual
431 mean value from the mean seasonal cycle (averaged value for each month across all
432 available years), anomalies are calculated as the deviation of a daily flux value from
433 the corresponding mean seasonal cycle.
434 A series of measures were used to assess the model performance (Kobayashi and
435 Salam, 2000; Jung et al., 2011; Tramontana et al., 2016).
436 The root mean square deviation (RMSD) reports the model accuracy by measuring
437 the differences between simulation and observation.
438 $$\mathrm{RMSD} = \sqrt{\frac{1}{n}\sum_{i=1}^{n}(x_i - y_i)^2}\ , \quad (9)$$
439 where x_i is simulated variable, y_i is measured variable, and n is the number of
440 observations.
441 Two signals (SDSD and LCS) are discriminated from the mean squared deviation
442 (Kobayashi and Salam, 2000). The squared difference (SDSD) between the standard
443 deviation of the simulation (SD_s) and the measurement (SD_m) shows if the model can
444 reproduce the magnitude of fluctuation among the n measurements.
445 $$\mathrm{SDSD} = (\mathrm{SD_s} - \mathrm{SD_m})^2; \text{with } \mathrm{SD_s} = \sqrt{\frac{1}{n}\sum_{i=1}^{n}(x_i - \bar{x})^2}\ , \mathrm{SD_m} = \sqrt{\frac{1}{n}\sum_{i=1}^{n}(y_i - \bar{y})^2}\ , \quad (10)$$
446 where $\bar{x}$ is simulated mean value, $\bar{y}$ is measured mean value.
447 The lack of correlation weighted by the standard deviations (LCS) is a measure to
448 examine if the model reproduces the observed phase of variability.
449 $$\mathrm{LCS} = 2\mathrm{SD_s}\mathrm{SD_m}(1 - r); \text{with } r = \left[\frac{1}{n}\sum_{i=1}^{n}(x_i - \bar{x})(y_i - \bar{y})\right] / (\mathrm{SD_s}\mathrm{SD_m})\ ,$$
450 (11)
451 where r is the Pearson's correlation coefficient.

Geosci. Model Dev. Discuss., https://doi.org/10.5194/gmd-2017-155
Manuscript under review for journal Geosci. Model Dev.
Discussion started: 7 September 2017

The Nash-Sutcliff modeling efficiency (MEF) is used to indicate the predictive accuracy of the model. MEF varies between negative infinity (–inf) and 1, an efficiency of 1 indicates a perfect fit between simulations and observations; an efficiency of 0 indicates the simulations are as accurate as the mean value of observations; a negative MEF indicates that mean value of observations has greater predictive power than the model.

$$\mathrm{MEF} = 1 - \frac{\sum_{i=1}^{n}(x_i - y_i)^2}{\sum_{i=1}^{n}(y_i - \bar{y})^2}, \quad (12)$$

4. Results

4.1 Site-specific V_{cmax} reduces errors in carbon simulations

Out of the 30 sites, 22 sites provided observed daily GPP (separated from measured NEE). The values of optimized V_{cmax} at each site were listed in Table 3. The optimized V_{cmax} varied from 19 to 89 μmol m^{-2} s^{-1} (Table 3), with a mean value of 40 μmol m^{-2} s^{-1}, which was higher than the default value (16 μmol m^{-2} s^{-1}) fixed by (Largeron et al., 2017).

Taylor diagrams were used to evaluate model results at these 22 sites (Fig. 3). The model had the best performance for GPP, with the correlation coefficient between simulated and observed GPP varied between 0.66 and 0.93 and all data points fell within the 0.9 root mean square difference circle. Simulated water table depth had a larger spread in correlation (0.16–0.82) and root mean square difference (0.4–4.0). We found no significant patterns of model-data misfits among different peatland types (fen, bog, others) or climate zones (temperate, boreal and arctic), as shown by different shapes or colors of markers in Fig. 3.

For the 22 sites where GPP observations were available, the modeled GPP errors were significantly reduced by optimizing V_{cmax} at each site (Table 4). When a fixed V_{cmax} value (16 μmol m^{-2} s^{-1}) was used, GPP was generally underestimated and across-sites differences were not reproduced (Fig. S3, Table 4). Unsurprisingly, neither the spatial nor the temporal variations of NEE were captured by the model when using the fixed V_{cmax} value (Fig. S3, Table 4). With site-specific V_{cmax} values

Geosci. Model Dev. Discuss., https://doi.org/10.5194/gmd-2017-155
Manuscript under review for journal Geosci. Model Dev.
Discussion started: 7 September 2017

(Site-by-site model performances are shown in Fig. S6 to S10 in Supplementary Materials), the overall (all the daily data from all the 22 sites) performance of the model was improved for GPP (r^2 = 0.76, MEF = 0.76), LE (r^2 = 0.42, MEF = 0.14), NEE (r^2 = 0.38, MEF = 0.26) and sensible heat (r^2 = 0.24, MEF = -0.50) (Fig. 4, Table 4). Seasonal variations in carbon and energy fluxes were generally well captured by the model (r^2 = 0.57 to 0.86). The spatial across-sites gradients of annual mean GPP, NEE and LE were generally good, with r^2 of 0.93, 0.27, and 0.71 and RMSDs of 0.41 g C m^{-2} day^{-1}, 0.60 g C m^{-2} day^{-1} and 9.85 W m^{-2}, respectively. The model performance was poor for predicting daily anomalies of all fluxes, with r^2 < 0.20. For both temporal and spatial variation, the MEF of the WT were negative, and r^2 smaller than 0.10, indicating that the model had the lowest predictive capability for the WT. Possible reasons for this could be: 1) peat management was not parameterized; i.e., the removal of beaver dams resulted in a decline of water level at US-Los; water level at US-WPT, CZ-Wet and RU-Che were manipulated; 2) the model diagnosed all peatland sites as fens by routing runoff from non-peatland areas into the peatland soil tile, whereas in the real world, bogs are only fed by precipitation. In other words, we included an extra water source for bogs than only rainfall; and 3) WT depends on water input from surrounding non-peatland areas, and the peatland area fraction derived from the map of Yu et al. (2010) could not represent the local area providing water for fens; 4) for global applications, the effects of micro-relief cannot be represented in the model, which has been proven to be an important regulator of the local hydrology cycle (Gong et al., 2012; Shi et al., 2015).

To better understand the influence of the water table dynamics on NEE in the model, we compared the second set of simulations (S2, the observed water table was used in the carbon module to define the fraction of oxic and anoxic decomposition in the acrotelm) with the first set (S1, the water table dynamics was calculated by the model). ORCHIDEE-PEAT showed only a small improvement in reproducing NEE when WT_{obs} was used (Table 5). To illustrate this effect, we took the Lompolojänkkä (FI-Lom) fen site as an example, in which WT was seriously underestimated (Fig. S8).

Geosci. Model Dev. Discuss., https://doi.org/10.5194/gmd-2017-155
Manuscript under review for journal Geosci. Model Dev.
Discussion started: 7 September 2017

While modeled WT varied between 5 and 54 cm below the surface, WT_{obs} was always above the soil surface. Fig. 5a showed that in comparison to S1, there was no aerobic respiration and larger anaerobic respiration in the acrotelm in S2. Due to the smaller acrotelm respiration (aerobic + anaerobic) in S2, there was larger carbon input from acrotelm to catotelm and consequently, there was more carbon accumulated in the catotelm in S2. Thus, the catotelm respiration in S2 was greater than in S1 (Fig. 5c), even though the catotelm respiration was very small. Because the growth of the peatland vegetation was not constrained by water in the model, the simulated GPP values were similar between S1 and S2 (Fig. 5a). With similar GPP but smaller soil respiration (the acrotelm + the catotelm respiration), S2 simulations thus resulted in more negative NEE values than S1 (higher net CO_2 uptake). Simulated leaf onset occurred earlier than observed at Lompolojänkkä site, causing the ecosystem switched from a carbon source to a carbon sink in May, while in observations the start of the carbon uptake was later (Fig. 5b). Although the model reproduced a similar amplitude of the observed NEE, the day-to-day variations of this flux were not captured (Fig. 6), causing an overestimation (more negative values) of NEE in the warm period (May-September).

4.2 Relationship between optimized V_{cmax} and meteorological variables

Several uni-variate ANOVA models were used to explain the spatial gradient of optimized V_{cmax}, explanatory variables including air temperature (T), precipitation (P), net radiation (NET_RAD), water use efficiency (WUE), water balance (WB) and the latitude (LAT). All explanatory variables were calculated as daily mean values during the growing season. Water use efficiency (g C m^{-2} mm^{-1} H_2O) was calculated as the ratio of GPP and evapotranspiration. Water balance (mm/day) was calculated as the difference between precipitation and evapotranspiration.

There was no significant difference between optimized V_{cmax} among peatland types (fen vs bog, $p = 0.16$), climate zones (temperate vs boreal vs arctic, $p = 0.17$), or dominant vegetation types (grasses and/or mosses dominated vs shrubs and/or trees

dominated, p = 0.67) (Fig. S4). However, we found a significant positive relationship between V_{cmax} and the growing season mean air temperature (Fig. S5, Table 6, r^2 = 0.19, $p < 0.05$) and a significant negative relationship between V_{cmax} and the latitude of the sites location (Fig. S5, Table 6, $r^2 = 0.23$, $p < 0.05$).

To verify the applicability of the empirical relationship found across sites between optimized V_{cmax} and the latitude (Fig. S5, slope = -0.92, intercept = 93.56, $r^2 = 0.23$, $p < 0.05$), we used the seven sites where there were no GPP observations available (US-Bes, DE-Hmm, US-Ics, PL-wet, SE-Sto, CA-Wp2 and CA-Wp3) as cross-validated sites. We compared model performance in simulating NEE with V_{cmax} being calculated according to the empirical relationship, and with V_{cmax} being fixed to its mean value of all 22 sites from Table 3 (40 μmol m^{-2} s^{-1}). The model performance in reproducing spatial gradients of NEE was improved when the V_{cmax} values derived from the empirical relationship were used (Fig. S11b, with RMSD reduced by 11%, r^2 increased from 0.20 to 0.38, and MEF increased from -0.04 to 0.17). This implies that compared to a fixed V_{cmax}, the usage of V_{cmax} value from the empirical relationship can better capture spatial gradients of NEE. It is worth mentioning that the empirical relationship was built on climate conditions from the last two decades (1999-2015), and thus may change in the future when the climate changes.

4.3 Soil temperature and a snow depth underestimation in the model

For most of the sites, soil temperature was underestimated in winter and overestimated in summer by our model (Fig. 7 and 8, results from sites DK-Nuf and CA-Wp1). One possible reason for the underestimation of soil temperature in winter is the underestimation of a snow depth (Fig. 9), since snow insulates the soil changing thermal conditions in comparison to a snow-free surface. The underestimation of the snow depth can be caused by the bias in snow processes of the model, such as overestimation of a snow density and subsequently overestimation of snow compaction, and/or overestimation of its sublimation. The insulation effects of the moss layer and the top organic layer are not included in this study, which may explain

why soil temperature was overestimated in summer but underestimated in winter. ORCHIDEE-PEAT calculates one energy budget for the vegetation and soil columns in one grid cell. Key parameters used for solving the heat diffusion equations in the soil, such as soil heat capacity and thermal conductivity, were prescribed by the dominant soil texture in the grid cell (Gouttevin et al., 2012). Nevertheless, similar to the case of hydrology module, the three default (coarse, medium, fine) soil textures cannot represent thermal properties of a peat soil (Paavilainen and Päivänen, 1995; Abu-Hamdeh and Reeder, 2000).

5. Discussion

ORCHIDEE-PEAT grouped various peatland vegetations into one plant functional type (PFT). This PFT cannot represent the true vegetation composition (shrubs, sedges, mosses etc.) of peatlands. However, by optimizing the value of V_{cmax} at each site, we matched simulated GPP with observations so that we had good carbon input to the soil. The V_{cmax} values estimated in this study ranged from 19 to 89 μmol m^{-2} s^{-1}, these values were not fully comparable with those reported in field studies, or values which were used in other peatland models because it is more like a representation of an average of all plants growing in peatland. We found that optimized V_{cmax} had a significant positive relationship with temperature, and a significant negative relationship with the latitude of chosen peatland sites location. We speculated that this can be attributed to 1) length of growing season increases as latitude decreases, and temperature and incoming solar radiation, increases. Longer growing season may enhance vegetation productivity (Fang et al., 2003; Nemani et al., 2003; Piao et al., 2007); 2) with an adequate water supply, leaves open their stomata in response to warm environments, leading to a higher photosynthetic efficiency (Chapin III et al., 2011); 3) the influence of temperature on nutrient availability for plants. The decomposition of plant litter and the release of nitrogen can be enhanced by high temperature, although litter decomposition is also driven by soil moisture, vegetation composition, litter quality and their interactions with temperature (Aerts, 2006;

Cornelissen et al., 2007; Gogo et al., 2016). Because nitrogen is one key element in proteins that are involved in photosynthesis process, photosynthesis capacity is highly correlated to nitrogen availability (Evans, 1989; Takashima et al., 2004; Walker et al., 2014). Since the nitrogen cycle is not explicitly included in the ORCHIDEE-PEAT, the relationship between V_{cmax} and the latitude (and temperature) possibly reflected the impact of nitrogen on photosynthesis rates.

Previous studies have shown that peatland functioning may have contrasting responses to variations in water table depth. Among sites incorporated in our study, Aurela et al. (2007) reported that at the FI-Sii site, drought increased respiration and thus diminished NEE; Adkinson et al. (2011) reported that reduced water availability in 2006 constrained photosynthesis capacity at the rich fen CA-Wp3 and consequently suppressed NEE, while the poor fen CA-Wp2 did not show significant response to the lower water table; at CA-Wp1 site, Flanagan and Syed (2011) reported that both photosynthesis and respiration increased in response to the warmer and drier conditions; Hurkuck et al. (2016) stated that temperature and light played a more important role than water table depth in controlling respiration and photosynthesis at DE-Bou site. In field observations, the timing, duration and intensity of drought have a major impact on the responses of peatland ecosystems. Lund et al. (2012) demonstrated that at SE-Faj site, a relatively short but severe drought that occurred in the middle of growing season of 2006 amplified respiration while a long-lasting drought that occurred at the beginning of growing season of 2008 reduced GPP. Lafleur et al. (2005) and Sulman et al. (2009) concluded from their studies at CA-Mer and US-Los that wetter peatlands would show stronger relationship between respiration and water table than drier peatlands because in a narrow range of the upper soils, small increases in WT (shallower WT) can result in a large increase in a soil water content and therefore respiration decrease, while below a critical level, soil water content shows only small increase with increasing WT and respiration changes are not so pronounced. Sulman et al. (2010) found that wetter conditions decreased respiration at fens but increased respiration at bogs, mainly due to different vegetation

composition at these two types of peatland: the fen sites had more shrubs and sedges while the bog sites had more mosses. In this study, we didn't distinguish between fens and bogs, and growth of peatland vegetation was not constrained by soil water in the model, thus the sensitivity of GPP to WT fluctuations in observations was not included in the model. However, the model can reproduce the pattern that above a critical level (acrotelm depth), peat respiration decreases with increasing WT (shallower WT).

ORCHIDEE-PEAT adequately captured the daily, seasonal and across-sites annual variations in GPP (with r^2 = 0.75, 0.86, and 0.93, respectively), but were less able to reproduce variations in NEE (with r^2 = 0.38, 0.61, and 0.27, respectively). One possible cause is that in the two-layer soil carbon scheme, the dependence of soil respiration on temperature was parameterized as an exponential function of the soil layers-weighted average temperature (Text S1), the vertical temperature gradient in the soil profile was ignored by the model. While field studies have shown that soil temperature is one of the most important predictors of respiration and values of Q_{10} coefficient depend on the soil depth (Lafleur et al., 2005; D'Angelo et al., 2016). Another possible cause is that small-scale peatland surface heterogeneities are not included in the model, which may exert important influences on water and carbon cycles but has been a challenge for global land surface models (Gong et al., 2013; Cresto Aleina et al., 2016).

For sites where latent and sensible heat were measured, about half of them used closed/enclosed path, which may cause an underestimation of LE and H (Twine et al., 2000). We also need to note that ORCHIDEE-PEAT only diagnose energy fluxes on one grid-cell and not for each soil tile/PFT present in the same grid cell. A site-varied and/or time-varied correction of LE and H measurements to force energy balance closure, and parameterizations of an independent energy budget at peatland may be helpful for better comparison of simulated and observed energy fluxes at peatland.

6. Conclusions

We developed ORCHIDEE-PEAT to simulate soil hydrology and carbon dynamics in peatlands. The model was evaluated at 30 northern peatland sites (Europe, USA, Canada, Russia). The optimization of V_{cmax} reduced the errors in carbon simulations, generally, the model reproduced the spatial gradient and temporal variations in GPP and NEE well. Water table depth was poorly simulated, possibly due to uncertainties in water input from non-peatland areas in the grid cell, and lack of representation of micro-relief, as well as the lack of consideration of the human impacts. A significant relationship between V_{cmax} and latitude was found, which may be attributed to the influence of temperature on growing season length and nutrient availability. For NEE fluxes, improvement brought by forcing the carbon module to use observed WT values (WT_{obs}), instead of calculated by the model, is small, indicating that the influence of poorly simulated WT on NEE is small.

Our study shows that to reproduce spatial gradients of NEE for northern peatlands, an average V_{cmax} value is not sufficient. To represent a spatial gradient of carbon fluxes in large-scale simulations of northern peatlands, incorporating the nitrogen cycle in peatlands could be helpful, or, an empirical relationship between V_{cmax} and the latitude (temperature) may be used as a proxy of nitrogen availability. Effects of water table variations on soil carbon decomposition are modeled as the partitioning of the acrotelm layer into oxic and anoxic zone, but effects of water table changes on GPP are not modeled in this study. The model needs further improvement in case to include the influences of water table on photosynthesis and depth-dependent influences of soil temperature on soil respiration, as well as an independent energy budget for peatland in a future model version.

Competing interests

The authors declare that they have no conflict of interest

684

685 **Code availability**

686 The code of ORCHIDEE-PEAT will be available upon request. The SVN version of
687 the code branch is svn://forge.ipsl.jussieu.fr/orchidee/perso/chunjing.qiu/ORCHIDEE,
688 revision 4596. Please contact the corresponding author to obtain the model.

689

690 **Data availability**

691 Primary data and scripts used in the analysis and other supplementary information can
692 be obtained from the corresponding author upon request.

693
694
695
696

697 *Acknowledgements*

698 This study was supported by the European Research Council Synergy grant
699 ERC-2013-SyG-610028 IMBALANCE-P. We would like to thank all the PIs for
700 giving us permission to use the flux and ancillary data, and all the help and advices
701 they provided while we were preparing the manuscript. We thank the Polish National
702 Science Centre which provided funds for site Kopytkowo (PL-Kpt) under projects
703 UMO-2011/01/B/ST10/07550 and UMO-2015/17/B/ST10/02187, and the Department
704 of Energy for supporting measurements at Lost Creek fen (US-Los) through the
705 Ameriflux Network Management Project. We gratefully acknowledge the financial
706 support provided for La Guette site under the Labex VOLTAIRE
707 (ANR-10-LABX-100-01) and the PIVOTS project of the Région Centre – Val de
708 Loire ((ARD 2020 program and CPER 2015 -2020). Data from the Greenlandic sites
709 (DK-ZaF and DK-NuF) were provided by the Greenland Ecosystem Monitoring
710 Programme.

711
712

References

Abu-Hamdeh, N. H. and Reeder, R. C.: Soil thermal conductivity effects of density, moisture, salt concentration, and organic matter, Soil Sci. Soc. Am. J., 64(4), 1285–1290, 2000.

Adkinson, A. C., Syed, K. H. and Flanagan, L. B.: Contrasting responses of growing season ecosystem CO_2 exchange to variation in temperature and water table depth in two peatlands in northern Alberta , Canada, , 116, 1–17, doi:10.1029/2010JG001512, 2011.

Aerts, R.: The freezer defrosting: Global warming and litter decomposition rates in cold biomes, J. Ecol., 94(4), 713–724, doi:10.1111/j.1365-2745.2006.01142.x, 2006.

Aurela, M., Laurila, T. and Tuovinen, J. P.: The timing of snow melt controls the annual CO_2 balance in a subarctic fen, Geophys. Res. Lett., 31(16), 3–6, doi:10.1029/2004GL020315, 2004.

Aurela, M., Riutta, T., Laurila, T., Tuovinen, J.-P., Vesala, T., Tuittila, E.-S., Rinne, J., Haapanala, S. and Laine, J.: CO_2 exchange of a sedge fen in southern Finland—the impact of a drought period, Tellus B, 59(5), 826–837, 2007.

Aurela, M., Lohila, A., Tuovinen, J. P., Hatakka, J., Riutta, T. and Laurila, T.: Carbon dioxide exchange on a northern boreal fen, Boreal Environ. Res., 14(4), 699–710, doi:10.1093/treephys/tpn047, 2009.

Barabach, J.: The history of Lake Rzecin and its surroundings drawn on maps as a background to palaeoecological reconstruction, Limnol. Rev., 12(3), 103–114, doi:10.2478/v10194-011-0050-0, 2012.

Barr, A. G., Black, T. A., Hogg, E. H., Kljun, N., Morgenstern, K. and Nesic, Z.: Inter-annual variability in the leaf area index of a boreal aspen-hazelnut forest in relation to net ecosystem production, Agric. For. Meteorol., 126(3–4), 237–255, doi:10.1029/2002JD003011, 2004.

Best, M. J., Pryor, M., Clark, D. B., Rooney, G. G. and Essery, R. L. H.: Model Development The Joint UK Land Environment Simulator (JULES), model description – Part 1 : Energy and water fluxes, , 677–699, doi:10.5194/gmd-4-677-2011, 2011.

Botta, A., Viovy, N., Ciais, P., Friedlingstein, P. and Monfray, P.: A global prognostic

scheme of leaf onset using satellite data, Glob. Chang. Biol., 6(7), 709–725, doi:10.1046/j.1365-2486.2000.00362.x, 2000.

Boutin, C. and Keddy, P. A.: A Functional Classification of Wetland Plants, J. Veg. Sci., 4(5), 591–600, doi:10.2307/3236124, 1993.

Bubier, J. L., Smith, R., Juutinen, S., Moore, T. R., Minocha, R., Long, S. and Minocha, S.: Effects of nutrient addition on leaf chemistry, morphology, and photosynthetic capacity of three bog shrubs, Oecologia, 167(2), 355–368, doi:10.1007/s00442-011-1998-9, 2011.

Bui, V.: Photosynthetic Performance of Chamaedaphne calyculata after Twelve Years of Nutrient Addition at Mer Bleue Bog, Ontario, Canada, 2013.

Carsel, R. F. and Parrish, R. S.: Developing joint probability distributions of soil water retention characteristics, Water Resour. Res., 24(5), 755–769, 1988.

Chapin III, F. S., Matson, P. A. and Vitousek, P.: Principles of terrestrial ecosystem ecology, Springer Science & Business Media., 2011.

Chaudhary, N., Miller, P. A. and Smith, B.: Modelling Holocene peatland dynamics with an individual-based dynamic vegetation model, Biogeosciences Discuss., (December), 1–46, doi:10.5194/bg-2016-319, 2016.

Chaudhary, N., Miller, P. A. and Smith, B.: Modelling past, present and future peatland carbon accumulation across the pan-Arctic, Biogeosciences Discuss., (February), 1–45, doi:10.5194/bg-2017-34, 2017.

Chojnicki, B. H., Urbaniak, M., Józefczyk, D., Augustin, J. and Olejnik, J.: Measurements of gas and heat fluxes at Rzecin wetland, Wetl. Monit. Model. Manag. Taylor Fr. Group, London, 125–131, 2007.

Chu, H., Chen, J., Gottgens, J. F., Ouyang, Z., John, R., Czajkowski, K. and Becker, R.: Net ecosystem methane and carbon dioxide exchanges in a Lake Erie coastal marsh and a nearby cropland, J. Geophys. Res. Biogeosciences, 119(5), 722–740, 2014.

Chu, H., Gottgens, J. F., Chen, J., Sun, G., Desai, A. R., Ouyang, Z., Shao, C. and Czajkowski, K.: Climatic variability, hydrologic anomaly, and methane emission can turn productive freshwater marshes into net carbon sources, Glob. Chang. Biol., 21(3),

769 1165–1181, doi:10.1111/gcb.12760, 2015.
770 Clymo, R. S.: The Limits to Peat Bog Growth, Philos. Trans. R. Soc. B Biol. Sci., 303(1117),
771 605–654, doi:10.1098/rstb.1984.0002, 1984.
772 Cornelissen, J. H. C., Van Bodegom, P. M., Aerts, R., Callaghan, T. V., Van Logtestijn, R. S.
773 P., Alatalo, J., Stuart Chapin, F., Gerdol, R., Gudmundsson, J., Gwynn-Jones, D., Hartley,
774 A. E., Hik, D. S., Hofgaard, A., Jónsdóttir, I. S., Karlsson, S., Klein, J. A., Laundre, J.,
775 Magnusson, B., Michelsen, A., Molau, U., Onipchenko, V. G., Quested, H. M., Sandvik, S.
776 M., Schmidt, I. K., Shaver, G. R., Solheim, B., Soudzilovskaia, N. A., Stenström, A.,
777 Tolvanen, A., Totland, Ø., Wada, N., Welker, J. M., Zhao, X., Brancaleoni, L.,
778 Brancaleoni, L., De Beus, M. A. H., Cooper, E. J., Dalen, L., Harte, J., Hobbie, S. E.,
779 Hoefsloot, G., Jägerbrand, A., Jonasson, S., Lee, J. A., Lindblad, K., Melillo, J. M., Neill,
780 C., Press, M. C., Rozema, J. and Zielke, M.: Global negative vegetation feedback to
781 climate warming responses of leaf litter decomposition rates in cold biomes, Ecol. Lett.,
782 10(7), 619–627, doi:10.1111/j.1461-0248.2007.01051.x, 2007.
783 Corradi, C., Kolle, O., Walter, K., Zimov, S. A. and Schulze, E. D.: Carbon dioxide and
784 methane exchange of a north-east Siberian tussock tundra, Glob. Chang. Biol., 11(11),
785 1910–1925, doi:10.1111/j.1365-2486.2005.01023.x, 2005.
786 Cresto Aleina, F., Runkle, B. R. K., Brücher, T., Kleinen, T. and Brovkin, V.: Upscaling
787 methane emission hotspots in boreal peatlands, Geosci. Model Dev., 9(2), 915–926,
788 doi:10.5194/gmd-9-915-2016, 2016.
789 D'Angelo, B., Gogo, S., Laggoun- Défarge, F., Le Moing, F., Jégou, F. and Guimbaud, C.:
790 Soil temperature synchronisation improves representation of diel variability of ecosystem
791 respiration in Sphagnum peatlands, Agric. For. Meteorol., 223(April), 95–102,
792 doi:10.1016/j.agrformet.2016.03.021, 2016.
793 Dawson, Q. L.: Low-lying agricultural peatland sustainability under managed water regimes,
794 October, (May) [online] Available from: http://hdl.handle.net/1826/1405, 2006.
795 Ducoudré, N. I., Laval, K. and Perrier, A.: SECHIBA, a New Set of Parameterizations of the
796 Hydrologic Exchanges at the Land-Atmosphere Interface within the LMD Atmospheric

General Circulation Model, J. Clim., 6, 248–273, doi:10.1175/1520-0442(1993)006<0248:SANSOP>2.0.CO;2, 1993.

Dušek, J., Čížková, H., Czerný, R., Taufarová, K., Šmídová, M. and Janouš, D.: Influence of summer flood on the net ecosystem exchange of CO2 in a temperate sedge-grass marsh, Agric. For. Meteorol., 149(9), 1524–1530, 2009.

Euskirchen, E. S., Bret-Harte, M. S., Scott, G. J., Edgar, C. and Shaver, G. R.: Seasonal patterns of carbon dioxide and water fluxes in three representative tundra ecosystems in northern Alaska, Ecosphere, 3(1), art4, doi:10.1890/ES11-00202.1, 2012.

Euskirchen, E. S., Edgar, C. W., Turetsky, M. R., Waldrop, M. P. and Harden, J. W.: Differential response of carbon fluxes to climate in three peatland ecosystems that vary in the presence and stability of permafrost, , 1576–1595, doi:10.1002/2014JG002683.Received, 2014.

Euskirchen, E. S., Shaver, G. R., Edgar, C. W. and Romanovsky, V. E.: Long-Term Release of Carbon Dioxide from Arctic Tundra Ecosystems in Alaska, Ecosystems, doi:10.1007/s10021-016-0085-9, 2016.

Evans, J. R.: Photosynthesis and nitrogen relationships in leaves of C3 plants, Oecologia, 78(1), 9–19, doi:10.1007/BF00377192, 1989.

Fang, J., Piao, S., Field, C. B., Pan, Y., Guo, Q., Zhou, L., Peng, C. and Tao, S.: Increasing net primary production in China from 1982 to 1999, Front. Ecol. Environ., 1(6), 293–297, 2003.

Flanagan, L. B. and Syed, K. H.: Stimulation of both photosynthesis and respiration in response to warmer and drier conditions in a boreal peatland ecosystem, Glob. Chang. Biol., 17(7), 2271–2287, doi:10.1111/j.1365-2486.2010.02378.x, 2011.

Fortuniak, K., Pawlak, W., Bednorz, L., Grygoruk, M., Siedlecki, M. and Zieliński, M.: Methane and carbon dioxide fluxes of a temperate mire in Central Europe, Agric. For. Meteorol., 232, 306–318, doi:10.1016/j.agrformet.2016.08.023, 2017.

Franz, D., Koebsch, F., Larmanou, E., Augustin, J. and Sachs, T.: High net CO2 and CH4 release at a eutrophic shallow lake on a formerly drained fen, Biogeosciences, 13(10),

3051–3070, doi:10.5194/bg-13-3051-2016, 2016.

Frolking, S., Roulet, N. T., Tuittila, E., Bubier, J. L., Quillet, A., Talbot, J. and Richard, P. J. H.: A new model of Holocene peatland net primary production, decomposition, water balance, and peat accumulation, Earth Syst. Dyn. Discuss., 1(1), 115–167, doi:10.5194/esdd-1-115-2010, 2010.

Frolking, S., Talbot, J., Jones, M. C., Treat, C. C., Kauffman, J. B., Tuittila, E.-S. and Roulet, N. T.: Peatlands in the Earth's 21st century climate system, Environ. Rev., 19(NA), 371–396, doi:10.1139/a11-014, 2011.

Van Genuchten, M. T.: A closed-form equation for predicting the hydraulic conductivity of unsaturated soils, Soil Sci. Soc. Am. J., 44(5), 892–898, 1980.

Gnatowski, T., Szatyłowicz, J., Brandyk, T. and Kechavarzi, C.: Hydraulic properties of fen peat soils in Poland, Geoderma, 154(3–4), 188–195, doi:10.1016/j.geoderma.2009.02.021, 2010.

Gogo, S., Laggoun- Défarge, F., Merzouki, F., Mounier, S., Guirimand-Dufour, A., Jozja, N., Huguet, A., Delarue, F. and Défarge, C.: In situ and laboratory non-additive litter mixture effect on C dynamics of Sphagnum rubellum and Molinia caerulea litters, J. Soils Sediments, 16(1), 13–27, doi:10.1007/s11368-015-1178-3, 2016.

Gong, J., Wang, K., Kellomäki, S., Zhang, C., Martikainen, P. J. and Shurpali, N.: Modeling water table changes in boreal peatlands of Finland under changing climate conditions, Ecol. Modell., 244(May), 65–78, doi:10.1016/j.ecolmodel.2012.06.031, 2012.

Gong, J., Kellomäki, S., Wang, K., Zhang, C., Shurpali, N. and Martikainen, P. J.: Modeling CO2 and CH4 flux changes in pristine peatlands of Finland under changing climate conditions, Ecol. Modell., 263, 64–80, doi:10.1016/j.ecolmodel.2013.04.018, 2013.

Gorham, E.: Northern peatlands: Role in the carbon cycle and probably responses to climate warming, Ecol. Appl., 1(2), 182–195, doi:10.2307/1941811, 1991.

Gouttevin, I., Krinner, G., Ciais, P., Polcher, J. and Legout, C.: Multi-scale validation of a new soil freezing scheme for a land-surface model with physically-based hydrology, Cryosphere, 6(2), 407–430, doi:10.5194/tc-6-407-2012, 2012.

853 Graniero, P. A. and Price, J. S.: The importance of topographic factors on the distribution of
854 bog and heath in a Newfoundland blanket bog complex, Catena, 36(3), 233–254,
855 doi:10.1016/S0341-8162(99)00008-9, 1999.
856 Hommeltenberg, J., Mauder, M., Drösler, M., Heidbach, K., Werle, P. and Schmid, H. P.:
857 Ecosystem scale methane fluxes in a natural temperate bog-pine forest in southern
858 Germany, Agric. For. Meteorol., 198, 273–284, doi:10.1016/j.agrformet.2014.08.017,
859 2014.
860 Hooijer, A., Page, S., Canadell, J. G., Silvius, M., Kwadijk, J., Wösten, H. and Jauhiainen, J.:
861 Current and future CO2 emissions from drained peatlands in Southeast Asia,
862 Biogeosciences, 7, 1505–1514, 2010.
863 Hurkuck, M., Brümmer, C. and Kutsch, W. L.: Near-neutral carbon dioxide balance at a
864 seminatural, temperate bog ecosystem, J. Geophys. Res. G Biogeosciences, 121(2),
865 370–384, doi:10.1002/2015JG003195, 2016.
866 Iversen, C. M., Sloan, V. L., Sullivan, P. F., Euskirchen, E. S., Mcguire, A. D., Norby, R. J.,
867 Walker, A. P., Warren, J. M. and Wullschleger, S. D.: The unseen iceberg: Plant roots in
868 arctic tundra, New Phytol., 205(1), 34–58, doi:10.1111/nph.13003, 2015.
869 Jung, M., Reichstein, M., Margolis, H. A., Cescatti, A., Richardson, A. D., Arain, M. A.,
870 Arneth, A., Bernhofer, C., Bonal, D., Chen, J., Gianelle, D., Gobron, N., Kiely, G., Kutsch,
871 W., Lasslop, G., Law, B. E., Lindroth, A., Merbold, L., Montagnani, L., Moors, E. J.,
872 Papale, D., Sottocornola, M., Vaccari, F. and Williams, C.: Global patterns of
873 land-atmosphere fluxes of carbon dioxide, latent heat, and sensible heat derived from eddy
874 covariance, satellite, and meteorological observations, J. Geophys. Res. Biogeosciences,
875 116(3), 1–16, doi:10.1029/2010JG001566, 2011.
876 Kleinen, T., Brovkin, V. and Schuldt, R. J.: A dynamic model of wetland extent and peat
877 accumulation: Results for the Holocene, Biogeosciences, 9(1), 235–248,
878 doi:10.5194/bg-9-235-2012, 2012.
879 Kobayashi, K. and Salam, M. U.: Comparing simulated and measured values using mean
880 squared desviation and its components, Agron. J., 92(March), 345–352,

881 doi:10.1007/s100870050043, 2000.
882 Krinner, G., Viovy, N., de Noblet-Ducoudré, N., Ogée, J., Polcher, J., Friedlingstein, P., Ciais,
883 P., Sitch, S. and Prentice, I. C.: A dynamic global vegetation model for studies of the
884 coupled atmosphere-biosphere system, Global Biogeochem. Cycles, 19(1), 1–33,
885 doi:10.1029/2003GB002199, 2005.
886 Lafleur, P. M., Moore, T. R., Roulet, N. T. and Frolking, S.: Ecosystem respiration in a cool
887 temperate bog depends on peat temperature but not water table, Ecosystems, 8(6), 619–629,
888 doi:10.1007/s10021-003-0131-2, 2005.
889 Laggoun-Défarge, F.,Gogo, S., Bernard-Jannin, L., Guimbaud, C., Zoccatelli, R., Rousseau,
890 J., Binet, S., D'Angelo, B., Leroy, F., Jozja, N., Le Moing, F., and , Défarge , C.: DOES
891 HYDROLOGICAL RESTORATION AFFECT GREENHOUSE GASES EMISSION
892 AND PLANT DYNAMICS IN SPHAGNUM PEATLANDS ?, Mires. Peat., 2016.
893 Largeron, C., Krinner, G., Ciais, P. and Brutel-Vuilmet, C.: Implementing northern peatlands
894 in a global land surface model: description and evaluation in the ORCHIDEE high latitude
895 version model (ORC-HL-PEAT), Geosci. Model Dev. Discuss., 2017, 1–26,
896 doi:10.5194/gmd-2017-141, 2017.
897 Letts, M. G., Roulet, N. T., Comer, N. T., Skarupa, M. R. and Verseghy, D. L.:
898 Parametrization of peatland hydraulic properties for the Canadian land surface scheme,
899 Atmosphere-Ocean, 38(1), 141–160, doi:10.1080/07055900.2000.9649643, 2000.
900 Lloyd, J. and Taylor, J. A.: On the temperature dependence of soil respiration, Funct. Ecol.,
901 315–323, 1994.
902 Lund, M., Lindroth, A., Christensen, T. R. and Ström, L.: Annual CO2 balance of a temperate
903 bog, Tellus B, 59(5), 804–811, 2007.
904 Lund, M., Christensen, T. R., Lindroth, A. and Schubert, P.: Effects of drought conditions on
905 the carbon dioxide dynamics in a temperate peatland, Environ. Res. Lett., 7(4), 45704,
906 2012.
907 Lund, M., Bjerke, J. W., Drake, B. G., Engelsen, O., Hansen, G. H., Parmentier, F.-J. W.,
908 Powell, T. L., Silvennoinen, H., Sottocornola, M., Tømmervik, H., Weldon, S. and Rasse,

D. P.: Low impact of dry conditions on the CO2 exchange of a Northern-Norwegian blanket bog, Environ. Res. Lett., 10(2), 25004, doi:10.1088/1748-9326/10/2/025004, 2015.

Malmer, N., Johansson, T., Olsrud, M. and Christensen, T. R.: Vegetation, climatic changes and net carbon sequestration in a North-Scandinavian subarctic mire over 30 years, Glob. Chang. Biol., 11(11), 1895–1909, doi:10.1111/j.1365-2486.2005.01042.x, 2005.

Mcgrath, M. J., Ryder, J., Pinty, B., Otto, J., Naudts, K., Valade, A., Chen, Y., Weedon, J. and Luyssaert, S.: A multi-level canopy radiative transfer scheme for ORCHIDEE (SVN r2566), based on a domain-averaged structure factor, , (November), doi:10.5194/gmd-2016-280, 2016.

McVeigh, P., Sottocornola, M., Foley, N., Leahy, P. and Kiely, G.: Meteorological and functional response partitioning to explain interannual variability of CO2 exchange at an Irish Atlantic blanket bog, Agric. For. Meteorol., 194, 8–19, doi:10.1016/j.agrformet.2014.01.017, 2014.

Merbold, L., Kutsch, W. L., Corradi, C., Kolle, O., Rebmann, C., Stoy, P. C., Zimov, S. A. and SCHULZE, E.: Artificial drainage and associated carbon fluxes (CO2/CH4) in a tundra ecosystem, Glob. Chang. Biol., 15(11), 2599–2614, 2009.

Mertens, S., Nijs, I., Heuer, M., Kockelbergh, F., Beyens, L., Kerckvoorde, A. Van and Impens, I.: Influence of High Temperature on End-of-Season Tundra CO2 Exchange, Ecosystems, 4(3), 226–236, doi:10.1007/s10021-001-0006-3, 2001.

Milecka, K., Kowalewski, G., Fiałkiewicz-Kozieł, B., Gałka, M., Lamentowicz, M., Chojnicki, B. H., Goslar, T. and Barabach, J.: Hydrological changes in the Rzecin peatland (Puszcza Notecka, Poland) induced by anthropogenic factors: Implications for mire development and carbon sequestration, The Holocene, 959683616670468, 2016.

Morris, P. J., Baird, A. J. and Belyea, L. R.: Bridging the gap between models and measurements of peat hydraulic conductivity, Water Resour. Res., 51(7), 5353–5364, 2015.

Mualem, Y.: A new model for predicting the hydraulic conductivity of unsaturated porous media, Water Resour. Res., 12(3), 513–522, 1976.

937 Nemani, R. R., Keeling, C. D., Hashimoto, H., Jolly, W. M., Piper, S. C., Tucker, C. J.,
938 Myneni, R. B. and Running, S. W.: Climate-driven increases in global terrestrial net
939 primary production from 1982 to 1999, Science., 300(5625), 1560–1563, 2003.
940 Nilsson, M., Sagerfors, J., Buffam, I., Laudon, H., Eriksson, T., Grelle, A., Klemedtsson, L.,
941 Weslien, P. E. R. and Lindroth, A.: Contemporary carbon accumulation in a boreal
942 oligotrophic minerogenic mire–A significant sink after accounting for all C-fluxes, Glob.
943 Chang. Biol., 14(10), 2317 – 2332, 2008.
944 Olefeldt, D., Roulet, N. T., Bergeron, O., Crill, P., Bäckstrand, K. and Christensen, T. R.: Net
945 carbon accumulation of a high-latitude permafrost palsa mire similar to permafrost-free
946 peatlands, Geophys. Res. Lett., 39(3), doi:10.1029/2011GL050355, 2012.
947 Orgeval, T., Polcher, J. and Rosnay, P. De: Sensitivity of the West African hydrological cycle
948 in ORCHIDEE to infiltration processes, Hydrol. Earth. Syst. Sc., 12(6), 1387–1401, 2008.
949 Orgeval, T. d': Impact du changement climatique sur le cycle de l'eau en Afrique de l'Ouest:
950 modélisation et incertitudes, modélisation et incertitudes. Diss., Paris 6, 2006.
951 Paavilainen, E. and Päivänen, J.: Peatland forestry: ecology and principles, Springer Science
952 & Business Media., 1995.
953 Page, S. E., Siegert, F., Rieley, J. O., Boehm, H.-D. V, Jaya, A. and Limin, S.: The amount of
954 carbon released from peat and forest fires in Indonesia during 1997, Nature, 420(6911),
955 61–65, 2002.
956 Page, S. E., Rieley, J. O. and Banks, C. J.: Global and regional importance of the tropical
957 peatland carbon pool, Glob. Chang. Biol., 17, 798–818,
958 doi:10.1111/j.1365-2486.2010.02279.x, 2011.
959 Parish, F., Sirin, A., Charman, D., Joosten, H., Minayeva, T., Silvius, M. and Stringer, L.:
960 Assessment on Peatlands, Biodiversity and Climate Change: Main Report., 2008.
961 Parmentier, F. J. W., van Huissteden, J., Van Der Molen, M. K., Schaepman‐Strub, G.,
962 Karsanaev, S. A., Maximov, T. C. and Dolman, A. J.: Spatial and temporal dynamics in
963 eddy covariance observations of methane fluxes at a tundra site in northeastern Siberia, J.
964 Geophys. Res. Biogeosciences, 116(G3), 2011.

Parton, W. J., Stewart, J. W. B. and Cole, C. V: Dynamics of C , N , P and S in grassland soils : a model, Biogeochemistry, 131(5), 109–131, 1988.

Piao, S., Friedlingstein, P., Ciais, P. and Viovy, N.: Growing season extension and its impact on terrestrial carbon cycle in the Northern Hemisphere over the past 2 decades, , 21, 1–11, doi:10.1029/2006GB002888, 2007.

Pirk, N., Sievers, J., Mertes, J., Parmentier, F.-J. W., Mastepanov, M. and Christensen, T. R.: Spatial variability of CO2 uptake in polygonal tundra - large overestimations by the conventional eddy covariance method, Biogeosciences Discuss., 2016, 1–18, doi:10.5194/bg-2016-537, 2016.

Reichstein, M., Falge, E., Baldocchi, D., Papale, D., Aubinet, M., Berbigier, P., Bernhofer, C., Buchmann, N., Gilmanov, T. and Granier, A.: On the separation of net ecosystem exchange into assimilation and ecosystem respiration: review and improved algorithm, Glob. Chang. Biol., 11(9), 1424–1439, 2005.

Rennermalm, A. K., Soegaard, H. and Nordstroem, C.: Interannual Variability in Carbon Dioxide Exchange from a High Arctic Fen Estimated by Measurements and Modeling, Arctic, Antarct. Alp. Res., 37(4), 545–556, doi:10.1657/1523-0430(2005)037[0545:IVICDE]2.0.CO;2, 2005.

Rezanezhad, F., Price, J. S., Quinton, W. L., Lennartz, B., Milojevic, T. and Van Cappellen, P.: Structure of peat soils and implications for water storage, flow and solute transport: A review update for geochemists, Chem. Geol., 429, 75–84, doi:10.1016/j.chemgeo.2016.03.010, 2016.

Riutta, T., Laine, J., Aurela, M., Rinne, J., Vesala, T., Laurila, T., Haapanala, S., Pihlatie, M. and TUITTILA, E.: Spatial variation in plant community functions regulates carbon gas dynamics in a boreal fen ecosystem, Tellus B, 59(5), 838–852, 2007.

Sagerfors, J., Lindroth, A., Grelle, A., Klemedtsson, L., Weslien, P. and Nilsson, M. B.: Annual CO2 exchange between a nutrient-poor, minerotrophic, boreal mire and the atmosphere, J. Geophys. Res. Biogeosciences, 113(1), 1–15, doi:10.1029/2006JDG000306, 2008.

993 Shi, X., Thornton, P. E., Ricciuto, D. M., Hanson, P. J., Mao, J., Sebestyen, S. D., Griffiths,
994 N. A. and Bisht, G.: Representing northern peatland microtopography and hydrology
995 within the Community Land Model, Biogeosciences, 12(21), 6463–6477,
996 doi:10.5194/bg-12-6463-2015, 2015.
997 Sottocornola, M., Laine, A., Kiely, G., Byrne, K. A. and Tuittila, E. S.: Vegetation and
998 environmental variation in an Atlantic blanket bog in South-western Ireland, Plant Ecol.,
999 203(1), 69–81, doi:10.1007/s11258-008-9510-2, 2009.
1000 Spahni, R., Joos, F., Stocker, B. D., Steinacher, M. and Yu, Z. C.: Transient simulations of
1001 the carbon and nitrogen dynamics in northern peatlands: From the Last Glacial Maximum
1002 to the 21st century, Clim. Past, 9(3), 1287–1308, doi:10.5194/cp-9-1287-2013, 2013.
1003 Strack, M., Waddington, J. M., Rochefort, L. and Tuittila, E. S.: Response of vegetation and
1004 net ecosystem carbon dioxide exchange at different peatland microforms following water
1005 table drawdown, J. Geophys. Res. Biogeosciences, 111(2), 1–10,
1006 doi:10.1029/2005JG000145, 2006.
1007 Stiegler, C., Lund, M., Røjle Christensen, T., Mastepanov, M. and Lindroth, A.: Two years
1008 with extreme and little snowfall: Effects on energy partitioning and surface energy
1009 exchange in a high-Arctic tundra ecosystem, Cryosphere, 10(4), 1395–1413,
1010 doi:10.5194/tc-10-1395-2016, 2016.
1011 Sulman, B. N., Desai, a. R., Cook, B. D., Saliendra, N. and Mackay, D. S.: Contrasting
1012 carbon dioxide fluxes between a drying shrub wetland in Northern Wisconsin, USA, and
1013 nearby forests, Biogeosciences, 6(6), 1115–1126, doi:10.5194/bg-6-1115-2009, 2009.
1014 Sulman, B. N., Desai, A. R., Saliendra, N. Z., Lafleur, P. M., Flanagan, L. B., Sonnentag, O.,
1015 MacKay, D. S., Barr, A. G. and Van Der Kamp, G.: CO2 fluxes at northern fens and bogs
1016 have opposite responses to inter-annual fluctuations in water table, Geophys. Res. Lett.,
1017 37(19), 3–7, doi:10.1029/2010GL044018, 2010.
1018 Takashima, T., Hikosaka, K. and Hirose, T.: Photosynthesis or persistence: Nitrogen
1019 allocation in leaves of evergreen and deciduous Quercus species, Plant, Cell Environ.,
1020 27(8), 1047–1054, doi:10.1111/j.1365-3040.2004.01209.x, 2004.

1021 Tramontana, G., Jung, M., Schwalm, C. R., Ichii, K., Camps-Valls, G., Ráduly, B.,
1022 Reichstein, M., Arain, M. A., Cescatti, A., Kiely, G., Merbold, L., Serrano-Ortiz, P.,
1023 Sickert, S., Wolf, S. and Papale, D.: Predicting carbon dioxide and energy fluxes across
1024 global FLUXNET sites with regression algorithms, Biogeosciences, 13(14), 4291–4313,
1025 doi:10.5194/bg-13-4291-2016, 2016.
1026 Turetsky, M., Wieder, K., Halsey, L. and Vitt, D.: Current disturbance and the diminishing
1027 peatland carbon sink, Geophys. Res. Lett., 29(11), 2002.
1028 Turunen, J., Tomppo, E., Tolonen, K. and Reinikainen, A.: Estimating carbon accumulation
1029 rates of undrained mires in Finland – application to boreal and subarctic regions, The
1030 Holocene, 12(1), 69–80, doi:10.1191/0959683602hl522rp, 2002.
1031 Twine, T. E., Kustas, W. P., Norman, J. M., Cook, D. R., Houser, P. R., Meyers, T. P.,
1032 Prueger, J. H., Starks, P. J. and Wesely, M. L.: Correcting eddy-covariance flux
1033 underestimates over a grassland, Agric. For. Meteorol., 103(3), 279–300,
1034 doi:10.1016/S0168-1923(00)00123-4, 2000.
1035 Vanselow-Algan, M., Schmidt, S. R., Greven, M., Fiencke, C., Kutzbach, L. and Pfeiffer, E.
1036 M.: High methane emissions dominated annual greenhouse gas balances 30 years after bog
1037 rewetting, Biogeosciences, 12(14), 4361–4371, doi:10.5194/bg-12-4361-2015, 2015.
1038 Walker, A. P., Beckerman, A. P., Gu, L., Kattge, J., Cernusak, L. A., Domingues, T. F.,
1039 Scales, J. C., Wohlfahrt, G., Wullschleger, S. D. and Woodward, F. I.: The relationship of
1040 leaf photosynthetic traits - Vcmax and Jmax - to leaf nitrogen, leaf phosphorus, and
1041 specific leaf area: A meta-analysis and modeling study, Ecol. Evol., 4(16), 3218–3235,
1042 doi:10.1002/ece3.1173, 2014.
1043 Wania, R., Ross, I. and Prentice, I. C.: Integrating peatlands and permafrost into a dynamic
1044 global vegetation model: 1. Evaluation and sensitivity of physical land surface processes,
1045 Global Biogeochem. Cycles, 23(3), 1–19, doi:10.1029/2008GB003412, 2009a.
1046 Wania, R., Ross, I. and Prentice, I. C.: Integrating peatlands and permafrost into a dynamic
1047 global vegetation model: 2. Evaluation and sensitivity of vegetation and carbon cycle
1048 processes, Global Biogeochem. Cycles, 23(3), 1–15, doi:10.1029/2008GB003413, 2009b.

1049 Williams, T. G. and Flanagan, L. B.: Measuring and modelling environmental influences on
1050 photosynthetic gas exchange in Spagnum and Pleurozium, Plant, Cell Environ., 21,
1051 555–564, doi:10.1046/j.1365-3040.1998.00292.x, 1998.
1052 Westergaard-Nielsen, A., Lund, M., Hansen, B. U. and Tamstorf, M. P.: Camera derived
1053 vegetation greenness index as proxy for gross primary production in a low Arctic wetland
1054 area, ISPRS J. Photogramm. Remote Sens., 86, 89–99, doi:10.1016/j.isprsjprs.2013.09.006,
1055 2013.
1056 Wright, I. J., Westoby, M., Reich, P. B., Oleksyn, J., Ackerly, D. D., Baruch, Z., Bongers, F.,
1057 Cavender-Bares, J., Chapin, T., Cornellissen, J. H. C., Diemer, M., Flexas, J., Gulias, J.,
1058 Garnier, E., Navas, M. L., Roumet, C., Groom, P. K., Lamont, B. B., Hikosaka, K., Lee, T.,
1059 Lee, W., Lusk, C., Midgley, J. J., Niinemets, Ü., Osada, H., Poorter, H., Pool, P.,
1060 Veneklaas, E. J., Prior, L., Pyankov, V. I., Thomas, S. C., Tjoelker, M. G. and Villar, R.:
1061 The worldwide leaf economics spectrum, Nature, 428, 821–827, doi:10.1038/nature02403,
1062 2004.
1063 Wu, Y., Verseghy, D. L. and Melton, J. R.: Integrating peatlands into the coupled Canadian
1064 Land Surface Scheme (CLASS) v3.6 and the Canadian Terrestrial Ecosystem Model
1065 (CTEM) v2.0, Geosci. Model Dev., 9(8), 2639–2663, doi:10.5194/gmd-9-2639-2016,
1066 2016.
1067 Yu, Z., Loisel, J., Brosseau, D. P., Beilman, D. W. and Hunt, S. J.: Global peatland dynamics
1068 since the Last Glacial Maximum, Geophys. Res. Lett., 37(13), 1–5,
1069 doi:10.1029/2010GL043584, 2010.
1070 Yurova, A., Wolf, A., Sagerfors, J. and Nilsson, M.: Variations in net ecosystem exchange of
1071 carbon dioxide in a boreal mire: Modeling mechanisms linked to water table position, J.
1072 Geophys. Res. Biogeosciences, 112(2), doi:10.1029/2006JG000342, 2007.
1073 Zhu, D., Peng, S., Ciais, P., Zech, R., Krinner, G., Zimov, S. and Grosse, G.: Simulating soil
1074 organic carbon in yedoma deposits during the Last Glacial Maximum in a land surface
1075 model, Geophys. Res. Lett., 43(10), 5133–5142, doi:10.1002/2016GL068874, 2016.
1076 Zona, D., Oechel, W. C., Kochendorfer, J., Paw U, K. T., Salyuk, A. N., Olivas, P. C.,

1077 Oberbauer, S. F. and Lipson, D. A.: Methane fluxes during the initiation of a large-scale
1078 water table manipulation experiment in the Alaskan Arctic tundra, Global Biogeochem.
1079 Cycles, 23(2), doi:10.1029/2009GB003487, 2009.
1080 Zobler, L.: A world soil file for global climate modeling. 1986, Natl. Aeronaut. Sp. Adm.
1081 Goddard Sp. Flight Center, Inst. Sp. Stud. NASA Tech. Memo., 87802, 32, 1986.
1082
1083
1084
1085
1086
1087
1088
1089
1090
1091
1092
1093
1094
1095
1096
1097
1098
1099
1100
1101
1102
1103
1104

Geosci. Model Dev. Discuss., https://doi.org/10.5194/gmd-2017-155
Manuscript under review for journal Geosci. Model Dev.
Discussion started: 7 September 2017

1105 **Figures and Tables**

1106

1107

1108

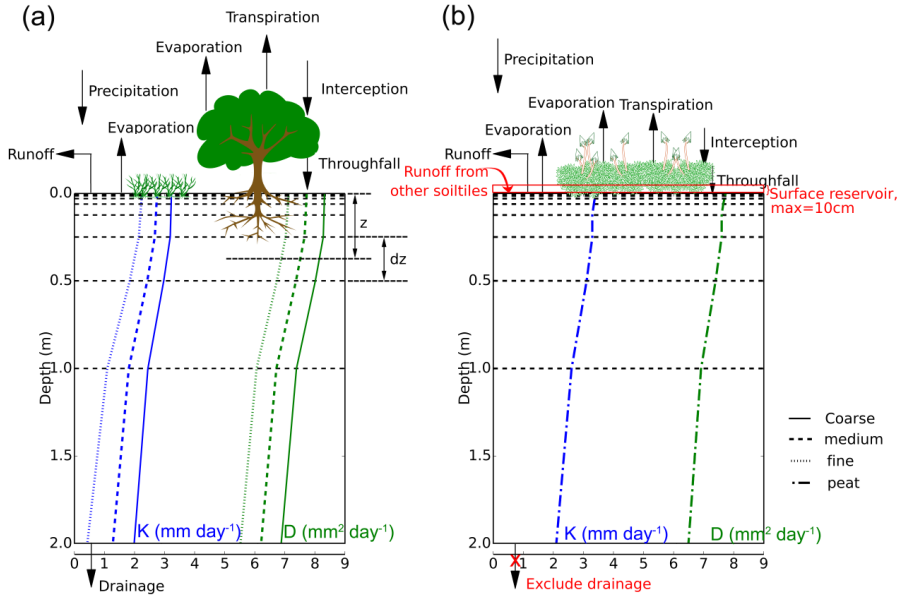

1109

1110 **Fig. 1.** Schematic of the hydrology module in ORCHIDEE. (a) water balance components in
1111 (a) a soil tile with either trees or grasses, (b) a peatland soil tile. Black dashed lines indicate
1112 the position of nodes in the eleven soil layers of the model. Blue lines: vertical profile of
1113 saturated hydraulic conductivity for different soil textures. Green lines: diffusivity for
1114 different soil textures. Vertical axis indicates soil depth, the horizontal axis indicates values
1115 of saturated hydraulic conductivity (K, mm day-1) and diffusivity (D, mm2 day-1), and scales
1116 are logarithmic based 10.

1117

1118

1119

1120

Geosci. Model Dev. Discuss., https://doi.org/10.5194/gmd-2017-155
Manuscript under review for journal Geosci. Model Dev.
Discussion started: 7 September 2017

Geoscientific Model Development Discussions
Open Access
EGU

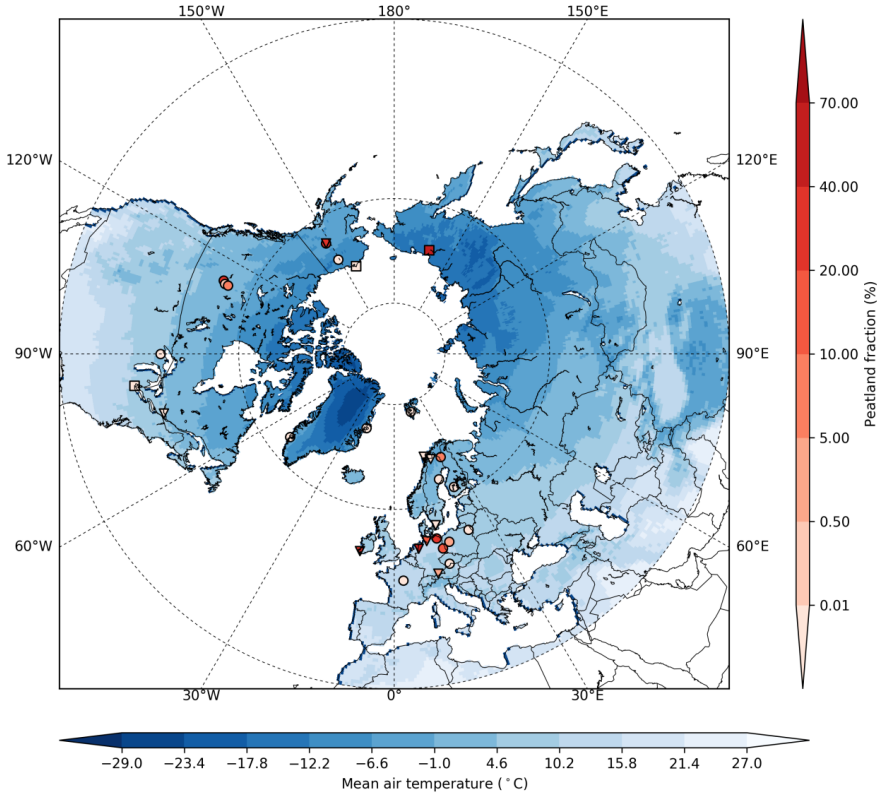

Fig. 2. The distribution of 30 peatland sites used in this study. Triangles are bogs; circles are fens; squares are tundra and marsh. Colors of the markers indicate peatland fractions in the 0.5 ° grid cell. Mean air temperatures is the annual mean from 1999 to 2015, based on the 6-hourly CRU-NCEP 0.5 °global database.

Geosci. Model Dev. Discuss., https://doi.org/10.5194/gmd-2017-155
Manuscript under review for journal Geosci. Model Dev.
Discussion started: 7 September 2017

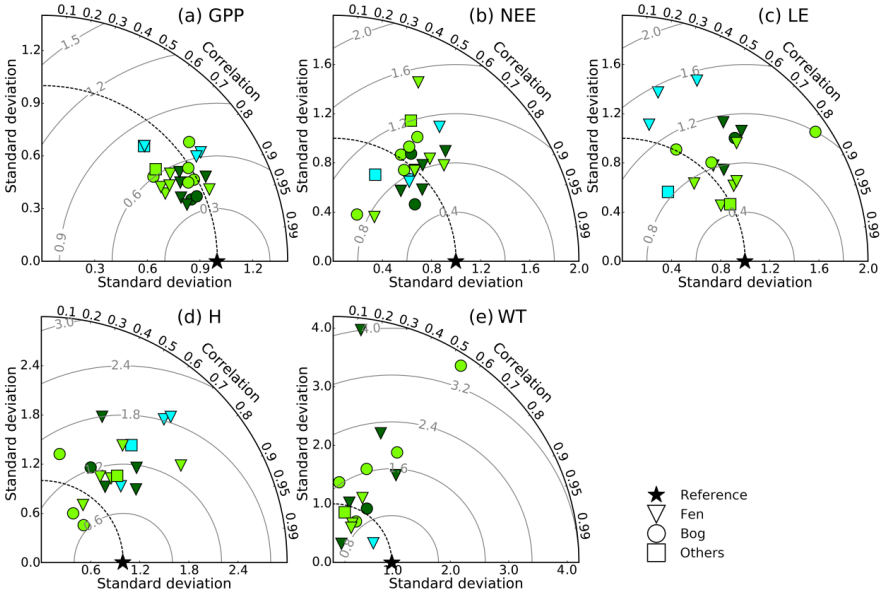

Fig. 3. Taylor diagrams of: (a) GPP (g C m-2 day-1); (b) NEE (g C m-2 day-1); (c) LE (W m-2); (d) H (W m-2) and (e) Water table depth (WT, cm). All statistics were calculated using daily averaged data. All points were normalized by dividing the standard deviation of model results by the standard deviation of the corresponding measurement, thus the reference point is 1.0. Light green markers represent temperate sites, dark green markers - boreal sites, blue markers - arctic sites.

Geosci. Model Dev. Discuss., https://doi.org/10.5194/gmd-2017-155
Manuscript under review for journal Geosci. Model Dev.
Discussion started: 7 September 2017

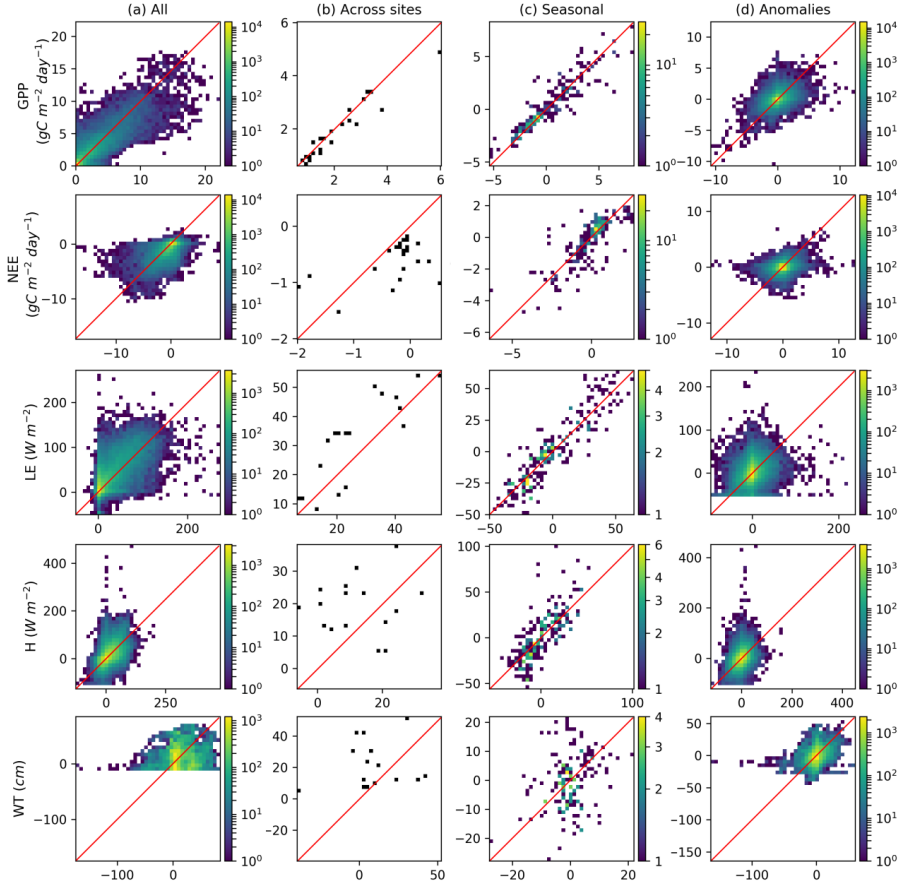

Fig. 4. Observed (x-axis) versus simulated (y-axis) fluxes (GPP, NEE, WT, LE, H) at the 22 sites where GPP derived from EC measurements were available. Fluxes were simulated using site-specific optimized Vcmax. The colors of points indicate the number of data in each bin, in panel (b) each data point represents one peatland site. The red line identifies the observations = the simulations.

Geosci. Model Dev. Discuss., https://doi.org/10.5194/gmd-2017-155
Manuscript under review for journal Geosci. Model Dev.
Discussion started: 7 September 2017

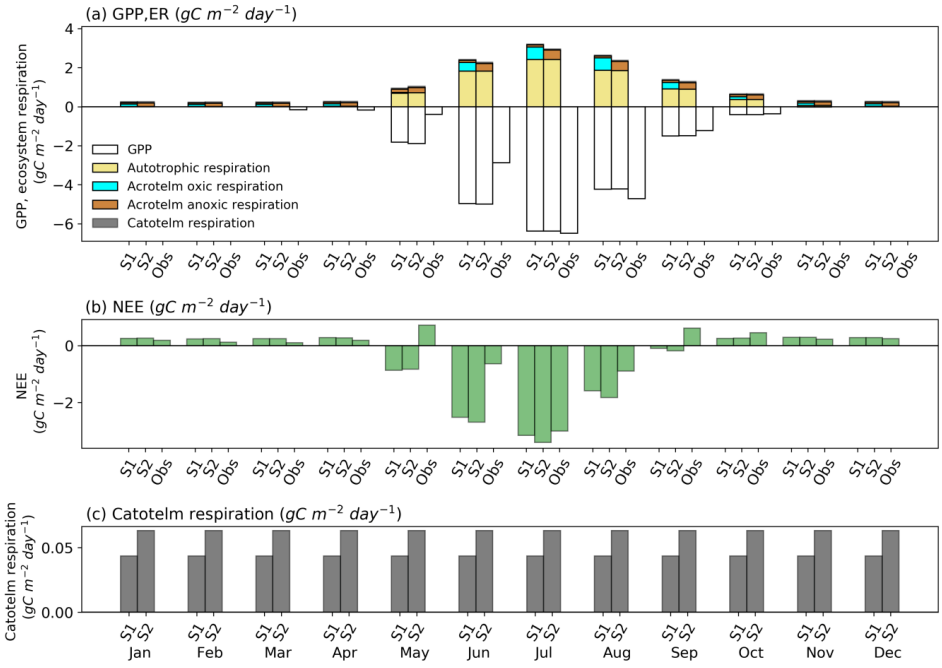

Fig. 5. Monthly mean (averaged over 2007–2009) of (a) GPP and ecosystem respiration(ER); (b) NEE; (c) catotelm respiration at Lompolojänkkä fen site (FI-Lom). S1: simulated water table (WT) was used in the carbon module; S2: observed WT values (WT_{obs}) was used; ob: measured NEE. The graph inserted shows catotelm respiration. By convention, a source of CO2 to the atmosphere is a positive number.

Geosci. Model Dev. Discuss., https://doi.org/10.5194/gmd-2017-155
Manuscript under review for journal Geosci. Model Dev.
Discussion started: 7 September 2017

Geoscientific Model Development Discussions

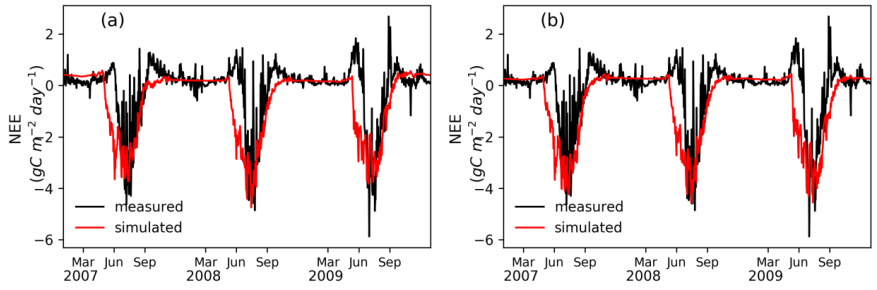

1168
1169

1170 **Fig. 6.** Observed and simulated daily mean NEE at FI-Lom fen site in a) S1 (Simulated WT
1171 was used in the carbon module); (b) S2 (modeled water table was assimilated to observed
1172 values (WT_{obs}) and was used in the carbon module).

1173
1174
1175
1176
1177
1178
1179
1180
1181
1182
1183
1184
1185
1186
1187
1188
1189
1190

Geosci. Model Dev. Discuss., https://doi.org/10.5194/gmd-2017-155
Manuscript under review for journal Geosci. Model Dev.
Discussion started: 7 September 2017

Geoscientific Model Development Discussions

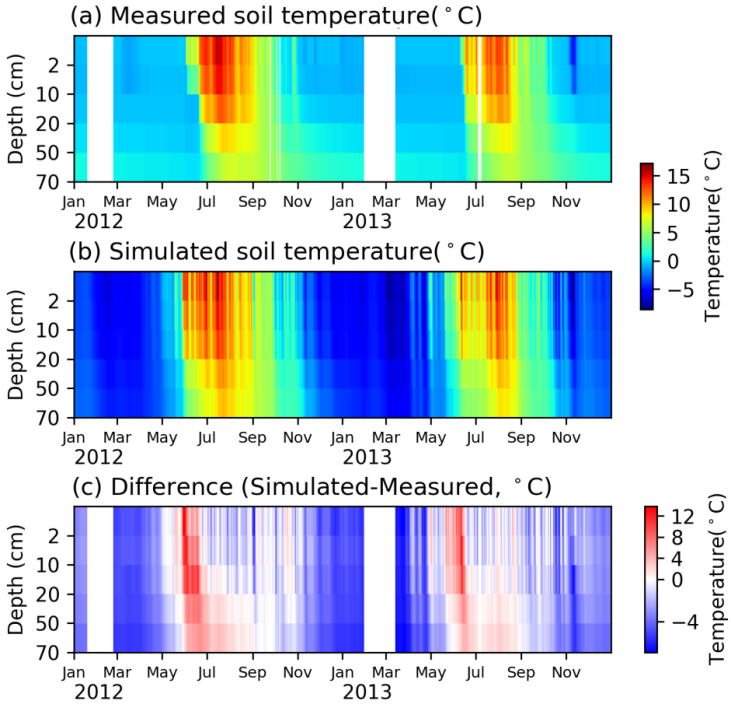

Fig. 7. Measured (a), simulated (b) soil temperature, and their difference (c) at DK-Nuf (64.13°, -51.39°) fen site. Soil temperature was measured at 2, 10, 20, 50 and 70 cm below soil surface. To compare simulated soil temperatures with the measurements, we linearly interpolated simulated soil temperature in different layers to the depths of the measurements.

Geosci. Model Dev. Discuss., https://doi.org/10.5194/gmd-2017-155
Manuscript under review for journal Geosci. Model Dev.
Discussion started: 7 September 2017

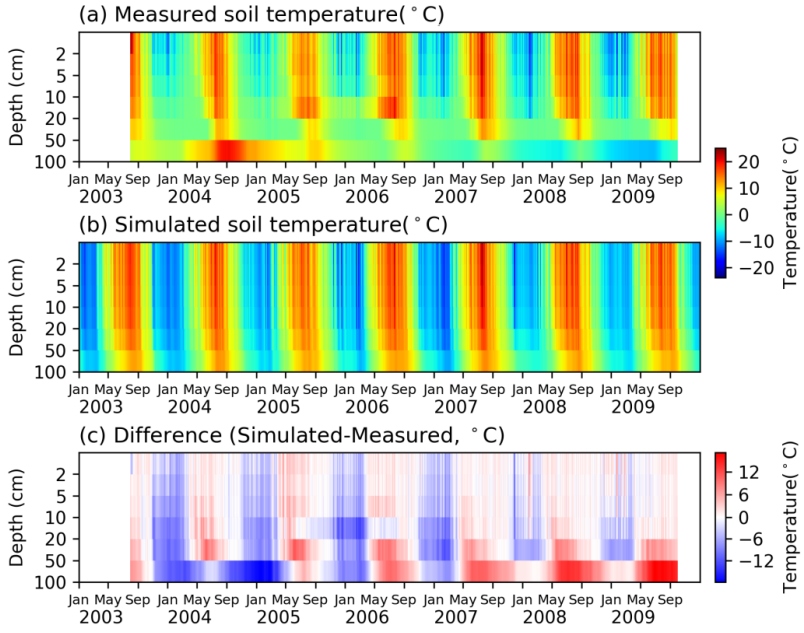

Fig. 8. Measured (a), simulated (b) soil temperature, and their difference (c) at CA-Wp1 (54.95°, -112.47°) fen site. The measured soil temperature (a) is the mean of a hummock and a hollow. Soil temperature was measured at 2, 10, 20, 50 and 100 cm below soil surface. To compare simulated soil temperatures with the measurements, we linearly interpolated simulated soil temperature in different layers to the depths of the measurements.

Geosci. Model Dev. Discuss., https://doi.org/10.5194/gmd-2017-155
Manuscript under review for journal Geosci. Model Dev.
Discussion started: 7 September 2017

Geoscientific Model Development Discussions

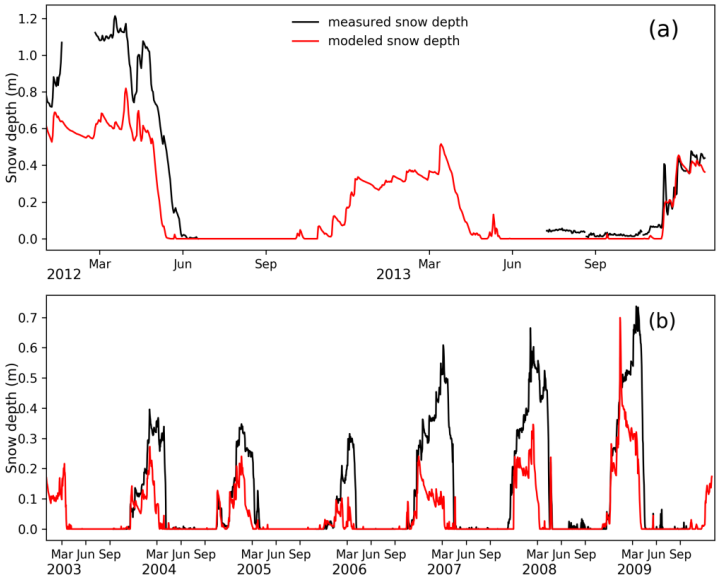

Fig. 9. Simulated versus measured snow depth (m) at (a) DK-Nuf fen and (b) CA-Wp1fen.

Geosci. Model Dev. Discuss., https://doi.org/10.5194/gmd-2017-155
Manuscript under review for journal Geosci. Model Dev.
Discussion started: 7 September 2017

Geoscientific Model Development Discussions

1225

1226 **Table 1.** Van Genuchten parameters used for different soil texture classes for non-peat soils
1227 (coarse, medium, fine), and for peat. θ_s is the saturated water content ($m^3\ m^{-3}$), θ_r is the
1228 residual water content ($m^3\ m^{-3}$); $K_{s\text{-}ref}$ is the reference saturated hydraulic conductivity ($m\ s^{-1}$);
1229 α is the inverse of the air entry suction (m^{-1}); *n* is a dimensionless parameter. In Eq. 1 and Eq.
1230 2, $m = 1\text{-}1/n$.
1231

	$K_{s\text{-}ref}$ ($m\ s^{-1}$)	*n*	α (m^{-1})	θ_s ($m^3\ m^{-3}$)	θ_r ($m^3\ m^{-3}$)
COARSE	1.23×10^{-5}	1.89	7.5	0.41	0.065
MEDIUM	2.89×10^{-6}	1.56	3.6	0.43	0.078
FINE	7.22×10^{-7}	1.31	1.9	0.41	0.095
PEAT	2.45×10^{-5}	1.38	5.07	0.90	0.15

Geosci. Model Dev. Discuss., https://doi.org/10.5194/gmd-2017-155
Manuscript under review for journal Geosci. Model Dev.
Discussion started: 7 September 2017

Geoscientific Model Development Discussions

Table 2. Sites Characteristics of the 30 peatlands (sites are sorted by latitude from south to north). The first column denotes if the site is used in the second set of simulation (S2, with water table prescribed in the model equal to observed values): y-YES, n-NO. Lat: latitude; Lon: longitude; MAT: long term mean annual air temperature; MAP: long term mean annual precipitation; Peatland fraction: fraction of peatland in the 0.5 ° grid cell which is read from the map of Yu et al. (2010), for cells where there is no peatland, mean fraction (22%) is used. Note that at US-Bog and US-Fen, the precipitation is growing season (from 16th May to 31th August) mean value, thus clarified as 'GS' in the table. Details of S2 and peatland fraction are provided in Sect. 3.3.

In S2	Code	Site name	Lat	Lon	climatic zone	Type	MAP (mm)	MAT (℃)	Elevation (m)	Peatland fraction (%)	Period	Citation
n	US-WPT	Winous Point North Marsh	41.46	-83.00	temperate	marsh	840	9.2	175	Mean (22)	2011-2013	Chu et al., 2014,2015
n	CA-Mer	Mer Bleue Eastern Peatland	45.41	-75.52	temperate	bog	944	6.0	70	Mean (22)	1999-2012	Lafleur et al.,2005
y	US-Los	Lost Creek	46.08	-89.98	temperate	fen	666	3.8	470	Mean (22)	2000-2010	Sulman et al., 2009
n	LA-GUE	La Guette peatland	47.32	2.27	temperate	fen	880	11.0	145	Mean (22)	2011-2013	D'Angelo et al.,2016; Laggoun-Défarge et al., 2016
y	DE-Sfn	Schechenfilz Nord	47.81	11.33	temperate	bog	1127	8.6	590	3.01	2012-2014	Hommeltenberg et al.,2014
y	CZ-Wet	CZECHWET	49.02	14.77	temperate	fen	614	7.4	426.5	Mean (22)	2007-2013	Dušek et al., 2009
n	DE-Spw	Spreewald	51.89	14.03	temperate	fen	559	9.5	61	11.01	2010-2014	

Geosci. Model Dev. Discuss., https://doi.org/10.5194/gmd-2017-155
Manuscript under review for journal Geosci. Model Dev.
Discussion started: 7 September 2017

y	IE-Kil	Killorglin-Glencar	51.97	-9.90	temperate	bog	2467	10.5	150	28.97	2002-2012	Sottocornola et al., 2009; McVeigh et al., 2014
y	DE-Bou	Bourtanger Moor	52.66	7.18	temperate	bog	799	10.0	19	63.98	2011-2014	Hurkuck et al., 2016
n	PL-Wet	Rzecin wetland	52.45	16.18	temperate	fen	526	8.5	54.	4.01	2006-2013	Chojnicki et al.,2007; Barabach, 2012; Milecka et al., 2017
n	PL-Kpt	Kopytkowo	53.59	22.89	temperate	fen	600	7.1	109	Mean (22)	2013-2015	Fortuniak et al., 2017
n	DE-Hmm	Himmelmoor	53.74	9.85	temperate	bog	838	9.0	12	15.99	2012-2014	Vanselow-Algan et al.,2015
n	DE-Zrk	Zarnekow	53.88	12.89	temperate	fen	584	8.7	<0.5	23.16	2013-2014	Franz et al., 2016
n	CA-Wp3	Western Peatland Rich Fen	54.47	-113.32	boreal	fen	504	2.1	670	29.77	2004-2006	Adkinson et al.,2011
n	CA-Wp1	Western Peatland	54.95	-112.47	boreal	fen	504	2.1	540	0.2	2003-2009	Flanagan and Syed, 2011
n	CA-Wp2	Western Peatland Poor Fen	55.54	-112.33	boreal	fen	504	2.1	730	8.07	2004-2006	Adkinson et al.,2011
y	SE-faj	Fäjemyr	56.27	13.55	temperate	bog	700	6.2	140	Mean (22)	2005-2009	Lund et al.,2007,2012
n	FI-Sii	Siikaneva	61.83	24.19	boreal	fen	713	3.3	162	Mean (22)	2005-2014	Aurela et al.,2007; Riutta et al., 2007
n	DK-NuF	Nuuk Fen	64.13	-51.39	arctic	fen	750	-1.4	40	Mean (22)	2008-2014	Westergaard-Nielsen et al., 2013

Geosci. Model Dev. Discuss., https://doi.org/10.5194/gmd-2017-155
Manuscript under review for journal Geosci. Model Dev.
Discussion started: 7 September 2017

Geoscientific Model Development Discussions
Open Access
EGU

y	SE-Deg	Degerö Stormyr	64.18	19.56	boreal	fen	523	1.2	270	Mean (22)	2001-2005	Sagerfors et al.,2008; Nilsson et al.,2008; Peichl et al., 2014
n	US-Bog	Alaska Bog	64.70	-148.32	boreal, thermokarst	bog	146 (GS)	-2.2	100	28.01	2011-2015	Euskirchen et al.,2014
n	US-Fen	Alaska Fen	64.70	-148.32	boreal	fen	146 (GS)	-2.2	100	28.01	2011-2015	Euskirchen et al.,2014
y	FI-Lom	Lompolojänkkä	68.00	24.21	boreal	fen	521	-1.0	269	5.08	2007-2009	Aurela et al.,2009
n	SE-Sto (ICOS)	Abisko Stordalen Palsa Bog	68.36	19.05	boreal, permafrost	bog	322	-0.14	360	Mean (22)	2014-2015	Malmer et al.,2005; Olefeldt et al.,2012
n	US-Ics	Imnavait Creek Watershed Wet Sedge Tundra	68.61	-149.31	arctic, permafrost	fen	318	-7.4	920	Mean (22)	2007-2011	Euskirchen et al.,2012, 2016
n	RU-Che	Cherskii	68.61	161.34	arctic, permafrost	tundra	200-215	-12.5	4	64.09	2002-2005	Corradi et al.,2005; Merbold et al., 2009
n	NO-And	Andøya	69.14	16.02	boreal	bog	1060	3.6	17	Mean (22)	2008-2014	Lund et al.,2015
n	US-Bes	Barrow-Bes (Biocomplexity Experiment South tower)	71.28	-156.60	arctic, permafrost	tundra	173	-12	4	Mean (22)	2005-2008	Zona et al.,2009
n	DK-Zaf	Zackenberg Fen	74.48	-20.55	arctic, permafrost	fen	211	-9.0	35	Mean (22)	2008-2011	Stiegler et al.,2016
n	NO-Adv	Adventdalen	78.19	15.92	arctic, permafrost	fen	190	-6.7	17	Mean (22)	2011-2014	Pirk et al., 2016

Geosci. Model Dev. Discuss., https://doi.org/10.5194/gmd-2017-155
Manuscript under review for journal Geosci. Model Dev.
Discussion started: 7 September 2017

Geoscientific Model Development Discussions

*For most of the sites, NEE was partitioned into GPP and ecosystem respiration following the nighttime partitioning method of , except that: NO-And used a light response curve approach following ; CA-Wp1 used the Fluxnet-Canada Research Network (FCRN) standard NEE partitioning procedure following ; and DE-Spw used the online gap filling and flux partitioning tool (http://www.bgc-jena.mpg.de/~MDIwork/eddyproc/) which uses the method proposed by

Geosci. Model Dev. Discuss., https://doi.org/10.5194/gmd-2017-155
Manuscript under review for journal Geosci. Model Dev.
Discussion started: 7 September 2017

Geoscientific Model Development Discussions
Open Access
EGU

Table 3. Optimized V_{cmax} (μmol m^{-2} s^{-1}) at each site.

Site	V_{cmax}	Site	V_{cmax}
US-WPT	80	FI-Sii	19
CA-Mer	25	DK-NuF	31
US-Los	65	SE-Deg	23
DE-Sfn	45	US-Bog	42
CZ-Wet	54	US-Fen	56
DE-spw	89	FI-Lom	28
IE-Kil	28	RU-che	35
DE-Bou	34	NO-And	21
DE-Zrk	33	DK-Zaf	37
CA-Wp1	38	NO-Adv	28
SE-faj	21	PL-Kpt	52

Geosci. Model Dev. Discuss., https://doi.org/10.5194/gmd-2017-155
Manuscript under review for journal Geosci. Model Dev.
Discussion started: 7 September 2017

Geoscientific Model Development Discussions

Table 4. Model performance measures for GPP, WT, NEE, LE and H. The left-hand column shows results with site-specific optimized V_{cmax} at each site, the right-hand column shows results with the fixed V_{cmax} (16 μmol m^{-2} s^{-1}) at all sites.

	Site-specific optimized V_{cmax}					Default V_{cmax} (constant value,16 μmol m^{-2} s^{-1})				
Flux	RMSD	SDSD	LCS	r^2	MEF	RMSD	SDSD	LCS	r^2	MEF
	Overall (Daily variability)					Overall (Daily variability)				
GPP	1.39	0.11	1.80	0.76	0.76	3.25	6.63	0.58	0.34	-0.33
NEE	1.30	0.02	1.56	0.38	0.26	1.47	1.91	0.20	0.19	0.03
LE	31.67	21.65	932.76	0.42	0.14	31.85	21.68	942.67	0.42	0.13
H	35.40	96.59	1151.28	0.24	-0.50	35.42	96.77	1153.52	0.24	-0.50
WT	25.93	10.26	661.80	0.01	-0.56	26.21	3.54	682.21	0.02	-0.59
	Across sites variability					Across sites variability				
GPP	0.41	0.03	0.10	0.93	0.89	2.29	1.28	0.18	0.08	-2.46
NEE	0.60	0.06	0.20	0.27	-0.01	0.65	0.33	0.02	0.02	-0.18
LE	9.85	1.13	65.49	0.71	0.50	9.78	0.90	63.89	0.71	0.51
H	14.31	2.67	155.85	0.01	-1.04	14.21	2.51	155.32	0.01	-1.01
WT	24.40	15.20	444.83	0.02	-0.82	25.39	3.57	464.55	0.04	-0.97
	Mean seasonal variability					Mean seasonal variability				
GPP	0.92	0.03	0.81	0.86	0.86	2.27	4.91	0.24	0.59	0.13
NEE	0.80	0.00	0.64	0.61	0.54	1.11	1.14	0.10	0.37	0.10
LE	11.49	7.75	124.23	0.83	0.78	11.79	7.63	131.38	0.82	0.77
H	17.85	65.77	252.65	0.57	0.11	17.86	63.66	255.26	0.56	0.11
WT	9.87	8.32	88.88	0.06	-1.38	10.00	13.84	86.04	0.11	-1.44
	Anomalies					Anomalies				
GPP	1.03	0.03	1.02	0.18	0.01	1.01	0.90	0.13	0.08	0.04
NEE	0.96	0.12	0.81	0.07	-0.07	0.92	0.76	0.09	0.01	0.01
LE	27.43	26.14	726.25	0.07	-0.94	27.56	26.90	732.60	0.06	-0.95
H	28.09	81.43	707.43	0.12	-1.12	28.16	83.17	709.65	0.12	-1.13
WT	13.25	0.40	174.69	0.10	-0.47	13.39	1.42	177.66	0.11	-0.50

Geosci. Model Dev. Discuss., https://doi.org/10.5194/gmd-2017-155
Manuscript under review for journal Geosci. Model Dev.
Discussion started: 7 September 2017

Geoscientific Model Development Discussions

Table 5. Model performance measures of NEE simulations for the site-by-site comparison, the comparison across sites, mean seasonal cycle and anomalies, using modeled (S1) and observed (S2) water table (WT).

	Modeled WT used (S1)					Observed WT used (S2)				
Site	RMSD	SDSD	LCS	r^2	MEF	RMSD	SDSD	LCS	r^2	MEF
CZ-Wet	2.97	3.61	4.38	0.46	0.37	2.86	3.22	4.27	0.50	0.41
DE-Bou	1.30	0.02	1.40	0.31	-0.21	1.31	0.03	1.41	0.31	-0.23
DE-Sfn	2.98	2.98	4.27	0.20	0.02	2.98	3.08	4.15	0.21	0.02
FI-Lom	1.05	0.01	0.94	0.46	0.21	1.08	0.02	0.95	0.49	0.16
IE-Kil	0.48	0.000	0.16	0.29	-0.37	0.49	0.002	0.16	0.32	-0.44
SE-Deg	0.64	0.03	0.33	0.51	0.09	0.57	0.01	0.29	0.51	0.26
SE-Faj	0.65	0.01	0.33	0.31	-0.36	0.65	0.02	0.33	0.32	-0.39
US-Los	3.15	0.05	8.78	0.47	-3.37	3.10	0.06	8.57	0.39	-3.23
Overall	1.95	0.20	3.52	0.02	-0.35	1.92	0.18	3.42	0.04	-0.31
Across sites	0.67	0.27	0.16	0.40	0.29	0.65	0.26	0.14	0.46	0.32
Seasonal	1.30	0.05	1.64	0.25	0.13	1.27	0.03	1.58	0.28	0.17
Anomalies	1.18	0.22	1.17	0.003	-0.34	1.17	0.21	1.17	0.001	-0.33

Geosci. Model Dev. Discuss., https://doi.org/10.5194/gmd-2017-155
Manuscript under review for journal Geosci. Model Dev.
Discussion started: 7 September 2017

Table 6. The results of the ANOVA analysis – the variance of optimized V_{cmax} in relation to chosen variables.

Variable	F-ratio	p-value	r^2 (%)
T	4.67	0.04*	18.95
P	0.95	0.34	4.52
NET_RAD	0.22	0.64	1.11
WUE	0.39	0.54	1.91
WB	1.35	0.26	6.32
LAT	6.08	0.023 *	23.30

* indicates statistical significance at a significance level of 0.05